# HIGHWAY RESEARCH RECORD

**Number 144**

## Pipe Culverts

3 Reports

Subject Classification

23 Highway Drainage
34 General Materials
62 Foundations (Soils)

HIGHWAY RESEARCH BOARD

DIVISION OF ENGINEERING NATIONAL RESEARCH COUNCIL
NATIONAL ACADEMY OF SCIENCES—NATIONAL ACADEMY OF ENGINEERING

Washington, D. C., 1966

Publication 1388

## *Department of Materials and Construction*

R. L. Peyton, Chairman
Assistant State Highway Engineer
State Highway Commission of Kansas, Topeka

HIGHWAY RESEARCH BOARD STAFF

R. E. Bollen, Engineer of Materials and Construction

W. G. Gunderman, Assistant Engineer of Materials and Construction

GENERAL MATERIALS DIVISION

John L. Beaton, Chairman
Materials and Research Engineer
Materials and Research Department
California Division of Highways, Sacramento

COMMITTEE ON CULVERTS AND CULVERT PIPE

(As of December 31, 1965)

Reynold K. Watkins, Chairman
Professor and Head
Mechanical Engineering Department
Utah State University, Logan

T. F. deCapiteau, Drainage Products Engineer, Manufacturing Division, Republic Steel Corporation, Youngstown, Ohio
W. B. Drake, Assistant State Highway Engineer for Planning, Research and Materials, Kentucky Department of Highways, Lexington
Kenneth S. Eff, Chief, Hydraulic Section, Civil Engineering Branch, Office, Chief of Engineers, Department of the Army, Washington, D.C.
C. J. Francis, Director, Engineering Division, Soil Conservation Service, U.S. Department of Agriculture, Washington, D.C.
R. T. Healy, Executive Secretary, Connecticut Concrete Pipe Association, Inc., South Windham
John G. Hendrickson, Jr., Water Resources Bureau, Portland Cement Association, Chicago, Illinois
A. H. Koepf, Consulting Engineer, Orinda, California
J. Alan Myers, Manager, Highway Construction Marketing, United States Steel Corporation, Pittsburgh, Pennsylvania
Eric Nordlin, Supervising Highway Engineer, Materials and Research Department, California Division of Highways, Sacramento
C. E. Proudley, Materials Consultant, Raleigh, North Carolina
E. P. Sellner, Hind Engineering Company, Highland Park, Illinois
Rockwell Smith, Research Engineer—Roadway, Association of American Railroads, Chicago, Illinois
M. G. Spangler, Civil Engineering Department, Iowa State University, Ames
Harold V. Swanson, Manager, Civil Engineering, International Pipe and Ceramics Corporation, Parsippany, New Jersey
H. L. White, Chief Engineer, Armco Metal Products Division, Armco Steel Corporation, Middletown, Ohio

# Foreword

Three papers are included in this RECORD, the first pertaining to the design of rigid conduits, the others concerning the structural failure of an 18.5-ft diameter corrugated steel culvert under an Interstate highway embankment in Montana. Two discussions and authors' closures accompany the latter two papers. This information will be of particular interest to designers and constructors of culverts, tunnels and underpasses under moderate and high fills.

In the first paper, Doubt analyzes the settlement ratio used in load formulas for positive projecting rigid conduits. This is defined as the ratio of the difference of the additional settlement of the critical plane in the exterior prism to the additional consolidation of the embankment material below the critical plane. The ratio is needed in determining the plane of equal settlement. The analytical derivation of the settlement ratio is based on the concept of a lower plane of equal settlement present either in the yielding foundation or at the upper surface of a nonyielding foundation. Expressions are derived for several typical examples of rigid conduits with different types and conditions in both yielding and nonyielding foundation materials.

Kraft and Eagle, representing the designers of the facility, present data on preliminary studies, design concepts, construction requirements and history of the corrugated steel structural plate culvert which was to carry a stream (3200 cfs design flow) under Interstate 15 in Wolf Creek Canyon between Helena and Great Falls, Montana. Maximum fill height was 83 ft with ⅜-in. thick steel plates under the heaviest fill. The authors analyze the bolt and seam strength requirements. Construction began in November 1963, the embankment reaching full height in the early spring of 1964. In mid-July two major breaks and displacements were noted in circumferential ring seams in the ⅜-in. plate with a 5-ft lateral displacement at midheight along one side of the pipe. Longitudinal seam failure also occurred. The overlapping plates moved past each other 4 to 5 ft reducing the culvert diameter to 16 ft. Many bolts were sheared and missing. The pipe was later uncovered and reconstructed with damaged plates and all bolts replaced. The imperfect trench method of backfill, considered but not used in the original construction, was employed in the reconstruction which has been in place since early 1966. A program was developed by Montana State University to check and evaluate the rebuilt structure. The designers mention possible causes of the culvert failure but present no conclusions.

Macadam presents results of research by his associates at Armco Steel, including laboratory simulation of joints. Based on the latter he concludes that A 490 bolts in the prototype were severely overtorqued, resulting in high bolt stress and ultimate failure, possibly at low temperatures with an environmental effect (such as corrosion) a factor. Among possible causes of the failure in the bolts, hydrogen embrittlement stress cracking is explored by Macadam. He states that the tests provide circumstantial evidence tending to support a corrosion-induced hydrogen-stress cracking hypothesis . . . which more closely matches the observed field conditions than do mechanisms attributable to . . . bolt weakness or overload.

Rumpf points out that the Engineering Foundation Research Council on Riveted and Bolted Structural Joints is investigating stress corrosion of high strength bolts and that no preliminary conclusions prejudicial to A 490 bolts for structural connections should be drawn at this time.

Spangler analyzes the culvert structural design using the classic principles of Marston's theory of loads on underground conduits. He concludes that the failure of the bolted longitudinal joints is due to the bolts being overstressed in shear and direct tension in lieu of attributing failure to the hypothesis of corrosion and hydrogen embrittlement. A factor is the low unit weight of 105 lb used in the design wherein the actual load was 130 lb/cu ft. He states that the rebuilt structure will apparently be safe although with a substantially lower safety factor than that sought in the original design.

In his closure, Macadam reaffirms importance of environmental effects as opposed to mechanical weakness or overstressing in explaining the bolt failures.

Eagle's closure states that the instrumentation in the rebuilt pipe indicates about 60 percent of the fill weight is being supported by the pipe, not the 100 percent theoretically possible. He concurs with Spangler's statement that the pipe may have been subject to greater loads than the design loads, but that the longitudinal seam strength was adequate.

The reader will find the widely differing theories as to the failure helpful in forming his own opinions. The designer will conclude that culvert structural analysis has not attained the perfection warranting reduction of safety factors and that a successful installation depends on careful construction practices.

# Contents

# Analysis for the Evaluation of the Settlement Ratio for Rigid Positive Projecting Conduits

PAUL D. DOUBT, Head, Design Unit, Engineering Division, Soil Conservation Service, U.S. Department of Agriculture, Hyattsville, Maryland

•THE SETTLEMENT ratio $\delta$ is a parameter used in load formulas of positive projecting conduits. Its value is required to determine the height of the plane of equal settlement $H_e$. The settlement ratio is defined as the ratio of the difference of the additional settlement of the top of the conduit and the additional settlement of the critical plane in the exterior prism to the additional consolidation of the embankment material below the critical plane.

$$\delta = \frac{(s_m + s_g) - (s_f + s_c)}{s_m} \tag{1}$$

where

- $s_m$ = additional consolidation of the embankment material in the exterior prism between the critical plane and the natural ground surface, ft;
- $s_g$ = additional settlement of the natural ground surface below the exterior prism due to the consolidation of the foundation, ft;
- $s_m + s_g$ = additional settlement of the critical plane in the exterior prism, ft;
- $s_c$ = additional deformation of the conduit, ft;
- $s_f$ = additional settlement of the bottom of the conduit (i.e., the surface of the natural ground beneath the conduit) due to the consolidation of the foundation, ft; and
- $s_f + s_c$ = additional settlement of the top of the conduit, ft.

The equation for determining the height of equal settlement $H_e$ is

$$e^{\pm 2K\mu(H_e/b_c)} \mp 2K\mu(H_e/b_c) = \pm 2K\mu\delta\rho + 1 \tag{2}$$

where

- $b_c$ = outside width of conduit, ft;
- $e$ = base of natural logarithms = 2.7183;
- $H_e$ = vertical distance from the plane of equal settlement to top of conduit, ft;
- $K$ = ratio at a point of active lateral pressure to vertical pressure for the backfill or embankment material;
- $\mu$ = tan $\phi$ = tangent of the angle of internal friction of the backfill or embankment material; and
- $\rho$ = projection ratio for positive projecting conduits = ratio of the distance between the natural ground surface and the top of the conduit (when $H_c = 0$) to the outside width of the conduit.

---

Paper sponsored by Committee on Culverts and Culvert Pipe and presented at the 45th Annual Meeting.

The value of $H_e$ can be determined from Eq. 2 if the values for $\delta$ and the other variables are known. The upper algebraic operation symbol is applicable for positive projecting conduits, and the lower algebraic operation symbol is to be used for negative projecting conduits.

The present method of estimating the value of $\delta$ is by judgment coupled with known boundary values. The value of $\delta$ can be determined after a conduit is installed (1), if provisions are made during the installation to obtain certain measurements.

The analytical derivation for the expression of $\delta$ presented herein is based on the concept of the existence of a lower plane of equal settlement either in the yielding foundation or at the upper surface of a nonyielding foundation. The existence of a lower plane of equal settlement can be shown by reasoning similar to that used by Marston (2) to prove the existence of an upper plane of equal settlement above the conduit. The parameters used in the derived expression of $\delta$ can be readily determined for the particular site conditions for which the conduit is installed.

## ASSUMPTIONS

The following assumptions are made in the derivation:

1. Vertical shearing planes exist adjacent to the cradle (or conduit if no cradle). The shearing plane is taken adjacent to the cradle because the total load on the cradle is to be evaluated. The additional load on the cradle is required to evaluate the additional settlements in the interior prism below the conduit.
2. Cohesion is negligible.
3. The magnitude of the shearing stresses is equal to the active lateral pressure at the vertical shearing planes multiplied by the tangent of the angle of internal friction of the embankment material.
4. The weight of the embankment material above the top of the conduit produces a uniform vertical pressure over the entire width of the interior prism.
5. The load on any horizontal differential element in the interior prism below the bottom of the conduit is a uniform vertical pressure over the entire width of the interior prism.
6. The shear at the sides of the interior prism is distributed as uniform vertical pressure (by virtue of internal friction in the embankment or foundation materials) over the entire width of the interior prism.
7. The shear at the sides of the exterior prism is distributed as uniform vertical pressures throughout the embankment and foundation in the infinitely wide exterior prism and its effect on the consolidation in the exterior prism may be neglected.
8. The embankment and foundation materials have constant moduli of consolidation.
9. The weight of the conduit and cradle are neglected.
10. One mathematical approximation is made in the derivation for case c and case d.

## SYMBOLS

The following additional symbols are used in the derivation:

$a = \dfrac{2K\mu}{b}$

$a_f = \dfrac{2K_f\mu_f}{b}$

$b$ = bottom width of cradle, ft. When no cradle is used, $b = b_c$ = outside width of conduit, ft;

$E$ = modulus of consolidation of the embankment material, tons/ft$^2$;

$E_f$ = modulus of consolidation of the foundation material, tons/ft$^2$;

$H$ = for the complete condition—vertical distance from top of backfill to a horizontal element of fill material having a height dH, ft; for the incomplete condition—vertical distance from plane of equal settlement to a horizontal element of fill material having a height dH, ft;

$H_c$ = vertical distance from top of backfill or embankment to top of conduit, ft;

$H'_e$ = distance between the top of the conduit and the upper plane of equal settlement when the interior prism has a width b;

$H_f$ = distance between the bottom of the cradle and the nonyielding foundation material, ft. When no cradle is used, it is the distance between the bottom of the conduit and the nonyielding foundation material.

$H_l$ = distance between the bottom of the cradle and the lower plane of equal settlement, ft. When no cradle is used, it is the distance between the bottom of the conduit and the lower plane of equal settlement;

$K_f$ = ratio at a point of active lateral pressure to vertical pressure on the foundation material;

$P'$ = vertical pressure on a horizontal plane within the interior prism when the embankment height is equal to or less than the height of equal settlement, lbs/ft length of conduit;

$P''$ = additional vertical pressure on a horizontal plane within the interior prism due to the weight of the material above the plane of equal settlement, lbs/ft length of conduit;

$\lambda_e$ = additional consolidation of the embankment material in the exterior prism between the critical plane and the plane of equal settlement, ft (positive projecting conduits);

$\lambda_i$ = additional consolidation of the embankment material in the interior prism between the top of the conduit and the plane of equal settlement, ft (positive projecting conduits);

$\mu_f$ = tangent of the angle of internal friction $\phi_f$ for the foundation material;

$\phi_f$ = angle of internal friction of the foundation material; and

$\Psi b_c$ = vertical distance between the natural ground line in the exterior prism and the bottom of the cradle (or the bottom of the conduit if no cradle is used), ft.

## CASES

The four cases represented by the drawings shown in Figures 1, 2, 3, and 5 will be considered separately.

Case a.

Value of $\delta$ for conduits resting on rock foundation. When the conduit and embankment are on nonyielding foundation (Fig. 1), the values of $s_g$, $s_c$ and $s_f$ are zero. Thus by Eq. 1

$$\delta = \frac{s_m}{s_m} = 1 \tag{3}$$

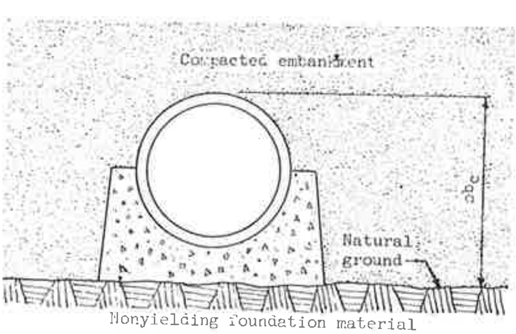


The surface of the nonyielding foundation is considered as the natural ground line. The distance between the top of the conduit and the natural ground line is $\rho b_c$.

Since the foundation is nonyielding, the additional settlements $s_f$ and $s_g$ are both zero, and

$$\delta = 1$$

Figure 1. Conduit resting in or on nonyielding foundations with embankment extending to the nonyielding foundation.

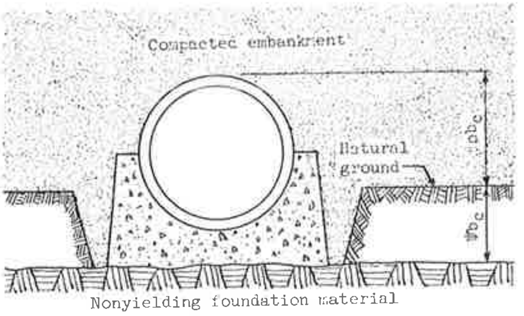


The value of $\delta$ is defined by the following relation

$$\delta = 1 + \left[\frac{\gamma_f}{\gamma}\frac{E}{E_f}\right]\frac{\Psi}{\rho}$$

Figure 2. Conduit resting on nonyielding support with compressible foundation materials adjacent to the conduit.

Case b.

Value of $\delta$ for conduits resting on rigid support with compressible adjacent foundation and embankment materials. When the conduit is on nonyielding foundation (Fig. 2), the values of $s_f$ and $s_c$ are zero.

$$\delta = \frac{(s_m + s_g)}{s_m} = 1 + \frac{s_g}{s_m}$$

The additional consolidation $s_m$ of the adjacent material between the top of the conduit and the natural ground is that consolidation due to the additional load. The additional load is the weight of the embankment between $H = H_c$ and $H = H'_e$ (Assumption 7)

$$s_m = \frac{\gamma(H_c - H'_e)}{E}\rho b_c \tag{4}$$

Similarly, the additional consolidation $s_g$ of the material between the natural ground and the bottom of the cradle is (Assumption 7)

$$s_g = \frac{\gamma(H_c - H'_e)}{E_f}\Psi b_c \tag{5}$$

On substituting these values of $s_m$ and $s_g$, obtain

$$\delta = 1 + \left[\frac{E}{E_f}\right]\frac{\Psi}{\rho} \tag{6}$$

Case c.

Determination of the settlement ratio $\delta$ when the foundation material below the top of the conduit is homogeneous material of sufficient depth (Fig. 3). By Eq. 15 when $s_c = 0$, the value of $\delta$ for rigid conduits is

$$\delta = \frac{s_m + s_g - s_f}{s_m} \tag{7}$$

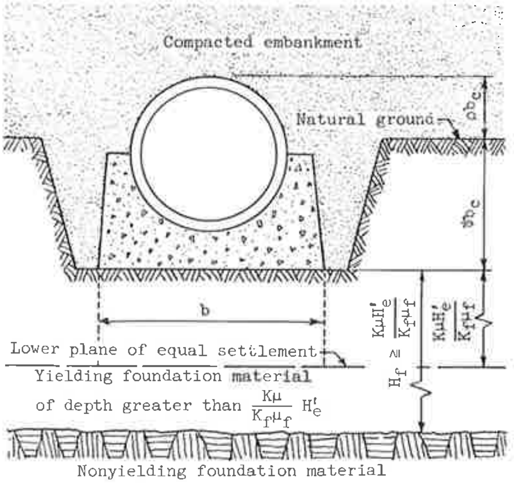


The values of $\delta$ and $H'_e$ are determined from the following two derived relations:

$$\delta = \frac{1 + \left[\frac{\gamma_f}{\gamma}\frac{E}{E_f}\right]\frac{\psi}{\rho}}{1 + \left[\frac{\gamma_f}{\gamma}\frac{E}{E_f}\right]\frac{K\mu}{K_f\mu_f}}$$

and

$$e^{2K\mu(H'_e/b)} - 2K\mu(H'_e/b) = 2K\mu\delta\rho + 1$$

When the value of $\delta$ has been determined from the first of these two relations, the value of $H'_e$ may be obtained from the second relation. The values of $\delta$ and $H'_e$ determined in this manner are the correct values of $\delta$ and $H'_e$ if $H_f \geq \frac{K\mu}{K_f\mu_f} H'_e$.

Figure 3. Conduit resting on yielding foundation material of sufficiently great depth.

But by definition the upper plane of equal settlement is the lowest horizontal plane at which the additional settlement at the plane for the top of the interior prism is equal to the settlement at the plane for the exterior prism, i.e.,

$$s_f + \lambda_i = s_g + \lambda_e + s_m \tag{8}$$

The evaluation of $s_f$, $s_g$, $s_m$, $\lambda_i$, and $\lambda_e$ is made later.

Lower plane of equal settlement. In the derivation of $\delta$ for this case, a lower plane of equal settlement is recognized. At this plane the intensities of pressure of the interior prism are equal to those of the exterior prism. Furthermore, the additional consolidation of every portion of each horizontal plane below this plane of equal settlement is equal. When loads are transferred into the upper interior prism, loads are transferred out of the lower interior prism. Thus, shearing forces of the upper interior prism are oppositely directed from those of the lower interior prism. The additional consolidation in the interior prism is equal to the additional consolidation in the exterior prism between the upper and lower planes of equal settlement when a rigid conduit is installed. Hence,

$$\lambda_i + \lambda'_i = \lambda_e + s_m + \lambda'_e \tag{9}$$

The evaluation of $\lambda$ involves the summation of the additional consolidations resulting from the variable additional pressures of each horizontal differential element. These pressures are evaluated next. The top sign in all of the following expressions pertains to the projection condition and the bottom sign pertains to the ditch condition.

Expressions for $P''_c$ and $P''_1$. Equating the vertical forces on the differential element $\Delta H$ (Fig. 4) for the interval $(H_c - H'_e) < H < H_c$

$$\frac{dP}{dH} \mp aP = \gamma b \tag{10}$$

where $P = P' + P''$.

For the interval $(H_c + \rho b_c + \Psi b_c) < H < (H_c + \rho b_c + \Psi b_c + H_1)$

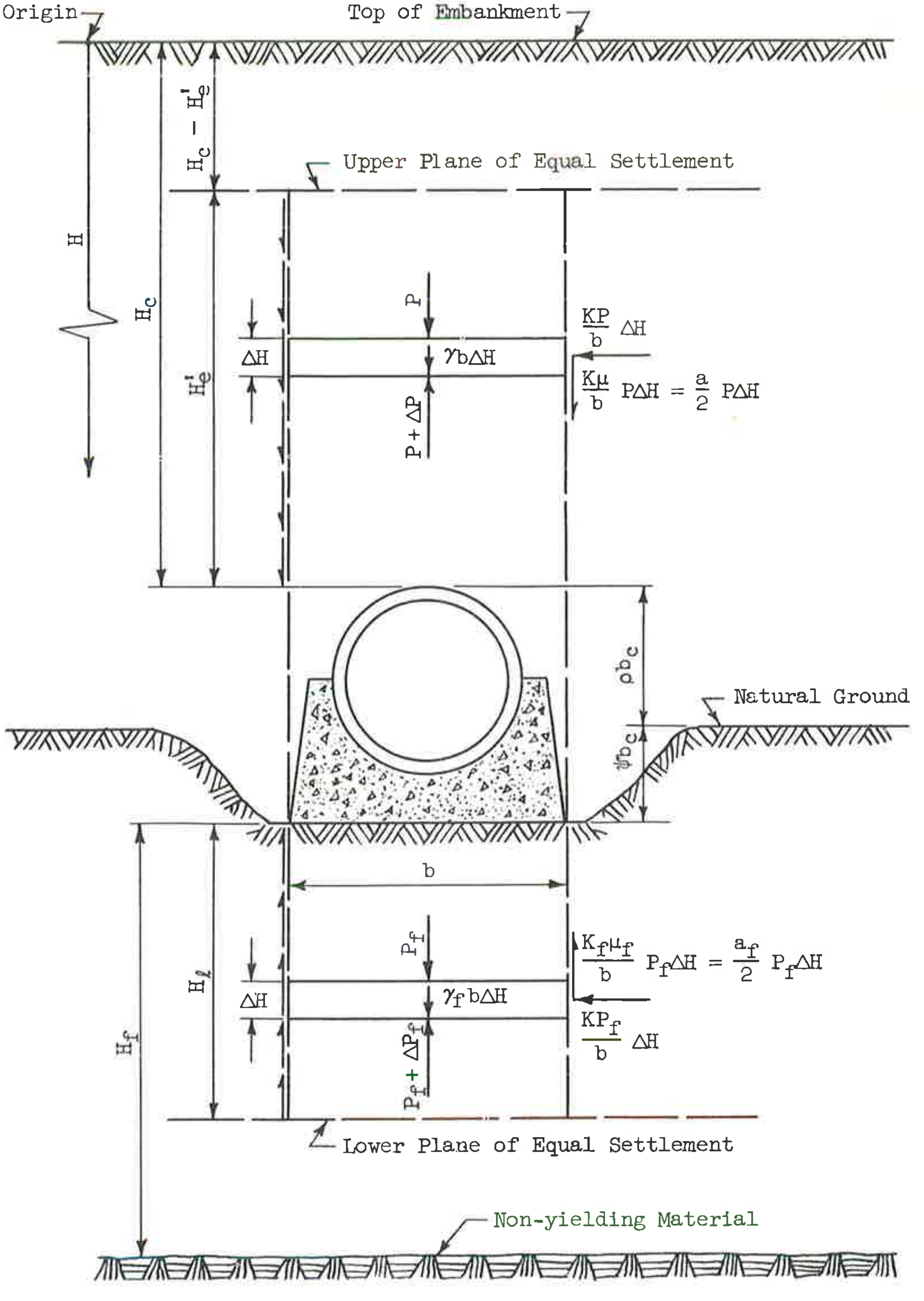


Figure 4. Analysis of settlement ratio δ.

$$\frac{dP}{dH} \pm a_f P = \gamma b \tag{11}$$

On observing the existence of the plane of equal settlement and since Eq. 10 is a linear homogenous differential equation, it may be written in two components

$$\frac{dP'}{dH} \mp aP' = \gamma b \tag{10a}$$

$$\frac{dP''}{dH} \mp aP'' = 0 \tag{10b}$$

and similarly Eq. 11 is written

$$\frac{dP'_1}{dH} \mp a_f P'_1 = \gamma b \tag{11a}$$

$$\frac{dP''_1}{dH} \mp a_f P''_1 = 0 \tag{11b}$$

The general solution of Eq. 10b is

$$P'' = c\, e^{\pm aH} \tag{12a}$$

where c is an arbitrary constant.

When $H = H_c - H'_e$, $P'' = \gamma b(H_c - H'_e)$, the value of c is

$$c = \gamma b(H_c - H'_e)\, e^{\mp a(H_c - H'_e)} \tag{12b}$$

At the top of the conduit $H = H_c$ and $P'' = P''_c$.

$$P'' = \gamma b(H_c - H'_e)\, e^{\pm aH'_e} \tag{13}$$

where $P''_c$ = additional vertical pressure on a horizontal plane at the top of the conduit.

The general solution of Eq. 11b is

$$P''_1 = c\, e^{\mp a_f H} \tag{14a}$$

where c is an arbitrary constant.

When $H = H_c + \rho b_c + \Psi b_c$, then $P''_1 = P''_c$, the value of c is

$$c = \gamma b(H_c - H'_e)\, e^{\pm\left[aH'_e + a_f(H_c + \rho b_c + \Psi b_c)\right]} \tag{14b}$$

At the lower plane of equal settlement $H = H_c + \rho b_c + \Psi b_c + H_l$ and $P'' = P''_1$

$$P''_1 = \gamma b(H_c - H'_e)\, e^{\pm(aH'_e - a_f H_l)} \tag{15}$$

where $P''_1$ = additional vertical pressure on a horizontal plane at the lower plane of equal settlement.

Expressions for $\lambda_e$, $\lambda_i$, $\lambda'_e$ and $\lambda'_i$. The differential equation expressing the additional consolidation in the interior prism $\lambda_i$ is

$$d\lambda_i = \frac{P''}{bE} dH$$

Substituting the value of $P''$ previously determined (Eqs. 12a and 12b)

$$d\lambda_i = \frac{\gamma}{E} (H_c - H'_e) e^{\pm a\left[H - (H_c - H'_e)\right]} dH$$

The general solution is

$$\lambda_i = \frac{\gamma}{E} (H_c - H'_e) e^{\mp a(H_c - H'_e)} \left[\frac{1}{\pm a} (e^{\pm aH} + c)\right] \tag{16a}$$

where c is an arbitrary constant.

When $H = H_c - H'_e$, then $\lambda_i = 0$, and the value of c is

$$c = - e^{\pm a (H_c - H'_e)} \tag{16b}$$

The total additional consolidation in the interior prism $\lambda_i$ between $H = H'_c - H'_e$ and $H = H_c$ is

$$\lambda_i = \frac{\gamma(H_c - H'_e)}{\pm aE} (e^{\pm aH'_e} - 1) \tag{17}$$

The additional consolidation in the exterior prism $\lambda_e$ for the interval $(H_c - H'_e) < H < H_c$ is

$$\lambda_e = \frac{\gamma(H_c - H'_e)}{E} H'_e \tag{18}$$

The differential equation expressing the additional consolidation in the lower interior prism $\lambda'_i$ is

$$d\lambda'_i = \frac{P''_1}{bE_f} dH$$

Substituting the value of $P''_1$ previously determined for Eqs. 14a and 14b, the general solution is

$$\lambda'_i = \frac{\gamma(H_c - H'_e)}{E_f} e^{\pm\left[aH'_e + a_f(H_c + \rho b_c + \Psi b_c)\right]} \left[\frac{1}{\mp a_f} (e^{\mp a_f H} + c)\right] \tag{19a}$$

where c is an arbitrary constant.

When $H = H_c + \rho b_c + \Psi b_c$, then $\lambda_i' = 0$, and the value of c is

$$c = -e^{\mp a_f(H_c + \rho b_c + \Psi b_c)} \tag{19b}$$

The total additional consolidation in the lower interior prism $\lambda_i'$ between $H = H_c + \rho b_c + \Psi b_c$ and $H = H_c + \rho b_c + \Psi b_c + H_l$ is

$$\lambda_i' = \frac{\gamma(H_c - H'_e)}{\pm a_f E_f} e^{\pm aH'_e}(1 - e^{\mp a_f H_l}) \tag{20}$$

The additional consolidation $\lambda'$ in the lower exterior prism is

$$\lambda_e' = \frac{\gamma(H_c - H'_e)}{E_f}(H_l + \Psi b_c) \tag{21}$$

The additional settlement $s_m$ of the material adjacent to the conduit is

$$s_m = \frac{\gamma(H_c - H'_e)}{E} \rho b_c \tag{4}$$

The expression for $H'_e$ is obtained by substituting the evaluations of $\lambda_i$ and $\lambda_e$ previously determined by Eqs. 17 and 18 into Eq. 8.

$$s_f + \frac{\gamma(H_c - H'_e)}{\pm aE}(e^{\pm aH'_e} - 1) = s_g + s_m + \frac{\gamma(H_c - H'_e)}{E} H'_e$$

Rearranging and using Eq. 1, $\delta s_m = s_m + s_g - s_f$

$$\delta \frac{\gamma(H_c - H'_e)}{E} \rho b_c = \frac{\gamma(H_c - H'_e)}{\pm aE}(e^{\pm aH'_e} - 1) - \frac{\gamma(H_c - H'_e)}{E} H'_e$$

which reduces to

$$e^{\pm aH'_e} - 1 = \pm a\delta\rho b_c \pm aH'_e$$

or

$$e^{\pm aH'_e} \mp aH'_e = \pm a\delta\rho b_c + 1 \tag{22}$$

This relation evaluates the position of the plane of equal settlement for the conduit and cradle. This relation differs from Eq. 2, which evaluates the plane of equal settlement for the conduit.

Expression for $H_l$. The location of the lower plane of equal settlement is determined by observing that the additional vertical pressure at the lower plane of equal settlement is equal to the additional vertical pressure at the upper plane of equal settlement.

$$\gamma(H_c - H'_e) b = \gamma b (H_c - H'_e) e^{\pm(aH'_e - a_f H_l)}$$

Rewriting

$$1 = e^{\pm(aH'_e - a_f H_l)} \tag{23}$$

or

$$aH'_e - a_f H_l = 0$$

and

$$H_l = \frac{a}{a_f} H'_e \tag{24}$$

Expression for evaluation of $\delta$. Substituting the evaluations of $s_m$, $\lambda_i$, $\lambda_e$, $\lambda'_i$ and $\lambda'_e$ as given by Eqs. 4, 17, 18, 20 and 21 into Eq. 9, obtain

$$\frac{\gamma(H_c - H'_e)}{\pm aE}(e^{\pm aH'_e} - 1) + \frac{\gamma(H_c - H'_e)}{\pm a_f E_f}\left[e^{\pm aH'_e} - e^{\pm aH'_e \mp a_f H_l}\right] =$$

$$\frac{\gamma(H_c - H'_e)}{E}(H'_e + \rho b_c) + \frac{\gamma(H_c - H'_e)}{E_f}(H_l + \Psi b_c) \quad \frac{\gamma(H_c - H'_e)}{\pm aE}$$

$$(e^{\pm aH'_e} - 1) + \frac{\gamma(H_c - H'_e)}{\pm a_f E_f} e^{\pm aH'_e}(1 - e^{\mp a_f H_l}) =$$

$$\frac{\gamma(H_c - H'_e)}{E}(\rho b_c + H'_e) + \frac{\gamma(H_c - H'_e)}{E_f}(H_l + \Psi b_c) \tag{25}$$

Multiplying by $\dfrac{\pm a}{H_c - H'_e}$ and substituting Eqs. 22 and 24, obtain on rearranging

$$\frac{\pm a\gamma}{E}(\delta\rho b_c + H'_e) + \frac{\gamma}{E_f}\frac{a}{a_f}\left[\pm a\delta\rho b_c \pm aH'_e\right] =$$

$$\frac{\pm a\gamma}{E}(H'_e + \rho b_c) \frac{\pm a\gamma}{E_f}\left[\frac{a}{a_f} H'_e + \Psi b_c\right]$$

On rearranging

$$\delta = \frac{1 + \left[\dfrac{E}{E_f}\right]\dfrac{\Psi}{\rho}}{1 + \left[\dfrac{E}{E_f}\right]\dfrac{a}{a_f}} \tag{26}$$

obtain

$$\delta = \frac{1 + \left[\frac{E}{E_f}\right]\frac{\Psi}{\rho}}{1 + \left[\frac{E}{E_f}\right]\frac{K\mu}{K_f\mu_f}} \tag{27}$$

Equation 27 gives the expression for $\delta$ when the foundation material is homogeneous for a sufficiently great depth. The depth $H_f$ is sufficiently great if $H_f \geq H_l$, or from Eq. 24, $H \geq \frac{K\mu}{K_f\mu_f} H'_e$.

Case d.

Determination of the settlement ratio $\delta$ when the foundation material is shallow ($H_f < H_l$). The additional settlements of the interior prism and exterior prisms for Case d at $H = H + (\rho + \Psi)\, b_c + H_f$ are equal. By the definition of the plane of equal settlement, the additional consolidations in the interior prism and exterior prisms between the plane of equal settlement and the nonyielding foundation are equal (Fig. 5). This results in the relation

$$\lambda'_i + \lambda_i = \lambda'_e + \lambda_e + s_m$$

The evaluations of the terms $s_m$, $\lambda_i$, and $\lambda_e$ are given by Eqs. 4, 17 and 18. The evaluations of $\lambda'_i$ and $\lambda'_e$ are obtained by substituting $H_f$ for $H_l$ in Eqs. 20 and 21. Making these substitutions, obtain

$$\frac{\gamma(H_c - H'_e)}{\pm a_f E_f}\, e^{\pm aH'_e}\left[1 - e^{\mp a_f H_f}\right] + \frac{\gamma(H_c - H'_e)}{\pm aE}\left[e^{\pm aH'_e} - 1\right] = \frac{\gamma(H_c - H'_e)}{E_f}(H_f + \Psi b_c) + \frac{\gamma(H_c - H'_e)}{E}(H'_e + \rho b_c)$$

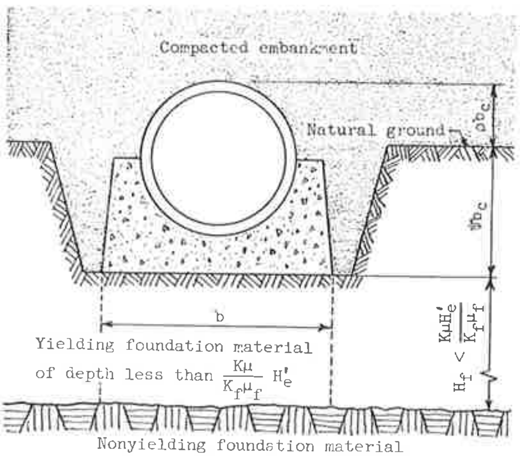


The values of $\delta$ and $H'_e$ depend, among other parameters, on the value of $H_f$. They are determined by the simultaneous solution of the following two derived relations:

$$\delta = \frac{1 + \left[\frac{\gamma_f}{\gamma}\frac{E}{E_f}\right]\frac{\psi}{\rho}}{1 + \left[\frac{\gamma_f}{\gamma}\frac{E}{E_f}\right]\frac{H_f}{H'_e}}$$

and

$$e^{2K\mu(H'_e/b)} - 2K\mu(H'_e/b) = 2K\mu\delta\rho + 1$$

Figure 5. Conduit resting on yielding foundation material of shallow depth.

Multiplying by $\frac{\pm a_f E_f}{\gamma(H_c - H'_e)}$ and substituting $xaH'_e$ for $a_f H_f$

$$e^{\pm aH'_e} \left[1 - e^{\mp axH'_e}\right] + \frac{a_f}{a}\frac{E_f}{E}\left[e^{\pm aH'_e} - 1\right] =$$

$$\pm(axH'_e + a_f \Psi b_c) \pm a_f \frac{E_f}{E}(H'_e + \rho b_c)$$

Recognizing that $e^{\pm aH'_e} - 1 = \pm a\delta\rho b_c \pm aH'_e$

$$\left[1 + \frac{a_f}{a}\frac{E_f}{E}\right]\left[\pm a\delta\rho b_c \pm aH'_e\right] + \left[1 - e^{\pm a(1 - x)H'_e}\right] =$$

$$\pm(axH'_e + a_f \Psi b_c) \pm a_f \frac{E_f}{E}(H'_e + \rho b_c)$$

or

$$\left[1 + \frac{a_f}{a}\frac{E_f}{E}\right](\delta\rho b_c) + \left\{\frac{1}{\pm a}\left[1 - e^{\pm a(1 - x)H'_e}\right] + (1 - x)H'_e\right\} =$$

$$\frac{a_f}{a}\Psi b_c + \frac{a_f}{a}\frac{E_f}{E}\rho b_c$$

Make the approximation

$$\frac{1}{\pm a}\left[1 - e^{\pm a(1 - x)H'_e}\right] + (1 - x)H'_e = (x - 1)\delta\rho b_c$$

Obtain

$$\left[x + \frac{a_f}{a}\frac{E_f}{E}\right](\delta\rho b_c) = \frac{a_f}{a}\Psi b_c + \frac{a_f}{a}\frac{E_f}{E}\rho b_c$$

or

$$\delta = \frac{1 + \left[\frac{E}{E_f}\right]\frac{\Psi}{\rho}}{1 + \left[\frac{E}{E_f}\right]\frac{H_f}{H'_e}} \qquad (28)$$

The simultaneous solution of Eqs. 2 and 28 can be given graphically. An illustration of such a graphical solution can be found in the technical publication of the Engineering Division of the Soil Conservation Service, Technical Release No. 5: The Structural Design of Underground Conduits.

## REFERENCES

1. Spangler, M. G. Field Measurements of the Settlement Ratios of Various Highway Culverts. Bull. 170, Iowa Engineering Experiment Station, Ames, 1950.
2. Marston, A. The Theory of External Loads on Close Conduits in the Light of the Latest Experiments. Bull. 96, Iowa Engineering Experiment Station, Ames, 1930.

# Design Features of an 18.5-Foot Diameter Culvert Installation in Montana and Data on Subsequent Failure

ALBERT N. KRAFT and HAROLD L. EAGLE, Morrison-Maierle, Inc., Helena, Montana

The natural topographic features of a winding mountainous canyon combined with additional restrictions imposed by an existing railroad and stream were the basic factors which influenced the alignment and grade selection for a portion of I15 in west central Montana. A profile requiring a 100-ft high fill, flanked by highway centerline cut depths of 175 ft and 95 ft on either side, dictated the selection of an enclosed pipe conduit to convey the canyon stream across I15. An 18.5-ft diameter structural plate circular pipe was selected and designed by the ring compression theory. The pipe was installed without instrumentation as part of a construction contract for 2.3 mi of Interstate highway.

Six months after initial completion of pipe fabrication, and two months after completion of the embankment over the pipe to full height, major ruptures in the pipe were discovered. The distressed condition of the pipe was so extreme as to require removal and reconstruction of a large portion of it.

This paper will present data covering physical features of the project site in their relationship to the selection of a pipe, basic design data and features of the pipe, and information and pictures of the failed pipe. A paper dealing with the examination of failed bolts taken from the culvert and special testing of the type of high strength bolts used in the culvert has been prepared by the Armco Steel Corporation.

•I15 IS THE only continuous north-south Interstate route through the state of Montana. Two of Montana's principal cities, Great Falls and Helena, lie 90 miles apart on the center portion of this route.

A study of several alternate locations to traverse the moderately elevated mountains between Helena and Great Falls resulted in the selection of the same canyon occupied by primary highway US 91, a spur line of the Great Northern Railway and a large creek.

The task of preparing a reconnaissance study for location of the Interstate, along with subsequent final design and plans preparation, was assigned to Morrison-Maierle Inc., Consulting Engineers, of Helena. A major decision was to use an earth fill approximately 100 ft high with a buried culvert at a particular crossing of Little Prickly Pear Creek (Fig. 1). The existing ground on one side consisted of a near-vertical solid rock face. The opposite side was also largely solid rock covered with talus and a thin soil mantle but with a natural ground slope of $1\frac{1}{4}$:1 (Fig. 2). Construction blasting procedures resulted in embankment rock pieces of under 1 cu yd in size for the most part. The borings taken at the culvert location revealed bedrock at a depth of 20 ft below the streambed and overlaid with silty sandy gravel.

Paper sponsored by Committee on Culverts and Culvert Pipe and presented at the 45th Annual Meeting.

Figure 1. Sketch of completed Interstate—note culvert.

## CULVERT REQUIREMENTS

The 50-yr design flow was established at 3200 cfs. Numerous design trials were made with various pipe types and sizes, invert slopes and multiple pipes. This resulted in the final selection of a single structural plate pipe of $18\frac{1}{2}$-ft diameter on an invert slope of 0.456 percent. Stream velocities with this slope would vary from 3 ft per sec at normal low flows of 25 to 50 cfs to 12.8 ft per sec at a flow of 3200 cfs. A camber of 0.4 ft was added at the quarter points. The use of this pipe size and slope resulted in the invert being placed 2 to 3 ft below the existing stream bed.

A reinforced concrete inlet headwall completely surrounding the pipe was used at right angles to the end of the pipe (Fig. 3). A 12-in. radius rounding of the inlet edges formed into the concrete was used to increase the capacity characteristic of the inlet. A reinforced concrete headwall was also used at the outlet, but it does not completely encircle the pipe. The top of it is 14 ft above the bottom of the pipe. It is tied into a concrete apron with a flat bottom and sloping sides which extend 15 ft beyond the end of the pipe. This structure provides protection to the abutments of a railroad bridge under which the pipe passes, and will prevent scour at the culvert outlet. Heavy riprap extends for another 63 ft beyond the apron where a concrete sill 32 ft long extending across the stream is located. The top of the concrete sill and the pipe outlet invert are at the same elevation, while the concrete and riprap aprons between the two are both 2 ft lower in elevation. This provides a pool and more resistance to scour at the outlet of the culvert.

Figure 2. Outlet end of culvert during construction.

Figure 3. Inlet end of culvert during construction.

A value of 105 lb per cu ft for the full vertical height of fill above the pipe was used for strength design. The actual weight of the embankment material, since it would be primarily rock, could be expected to be 130 lb per cu ft or more. However, considering the foundation material, the anticipated arching action in the rock embankment, and accepted practice in reduced unit weight for culvert design, the value to be used was established at 105 lb per cu ft.

A fill height over the pipe of 83 ft resulted in a unit load of 8.72 kips per sq ft. Considering the culvert as a compression ring, the load per foot of longitudinal seam was computed to be 76.6 kips, based on the reduced pipe diameter of 95 percent due to fabrication of the pipe to a 5 percent ellipsed shape. Standard 1 gage thick corrugated structural plate with the maximum number of standard bolts of 8 per lineal ft of seam provides an ultimate seam strength of 220,000 lb per lineal ft. This would provide a safety factor of 2.9. It was decided that this was too low for an installation of this magnitude and importance. Acceptable culvert practice has been based on the use of a safety factor of 4 for handbook type installations, where average backfilling practice is to be expected. On carefully controlled and well engineered installations a safety factor of 2 based on seam strength has been adequate in some cases. Test data furnished by the Armco Steel Corporation at the time of this design indicated that seam strength could be considerably increased with the use of corrugated $^3/_8$-in. thick ingot iron plate. Eight standard high-tensile $^3/_4$-in. ASTM A 325 bolts with 120,000 psi ultimate tensile strength provided an ultimate tested seam strength of 226,000 lb per lineal ft in this material. The use of 8 $^3/_4$-in. ASTM A 354 high strength bolts with 150,000 psi ultimate tensile strength resulted in an ultimate seam strength of 270,000 lb per lineal ft. The use of the latter combination was decided on since it provided a safety factor of 3.5.

To provide more latitude for bidding competitors, the seam strength requirement specified was for a minimum of 250,000 lb per lineal ft of seam, which would still supply a safety factor of 3.25. Proof, using actual test data showing that this strength could be attained, was required of the contractor. Proof submitted by the installer

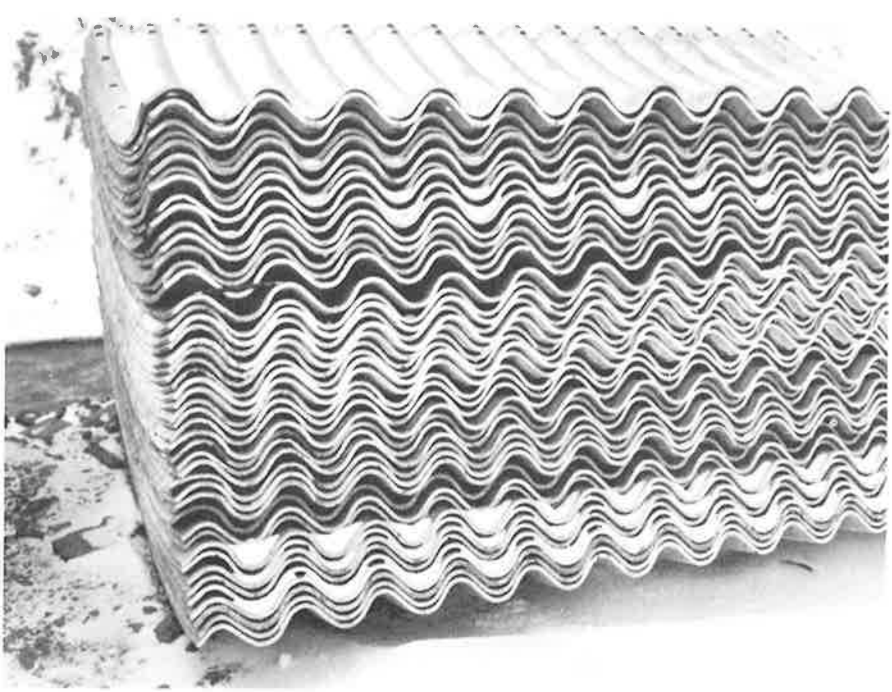

Figure 4. Edge view of pile of $^3/_8$-in. plates.

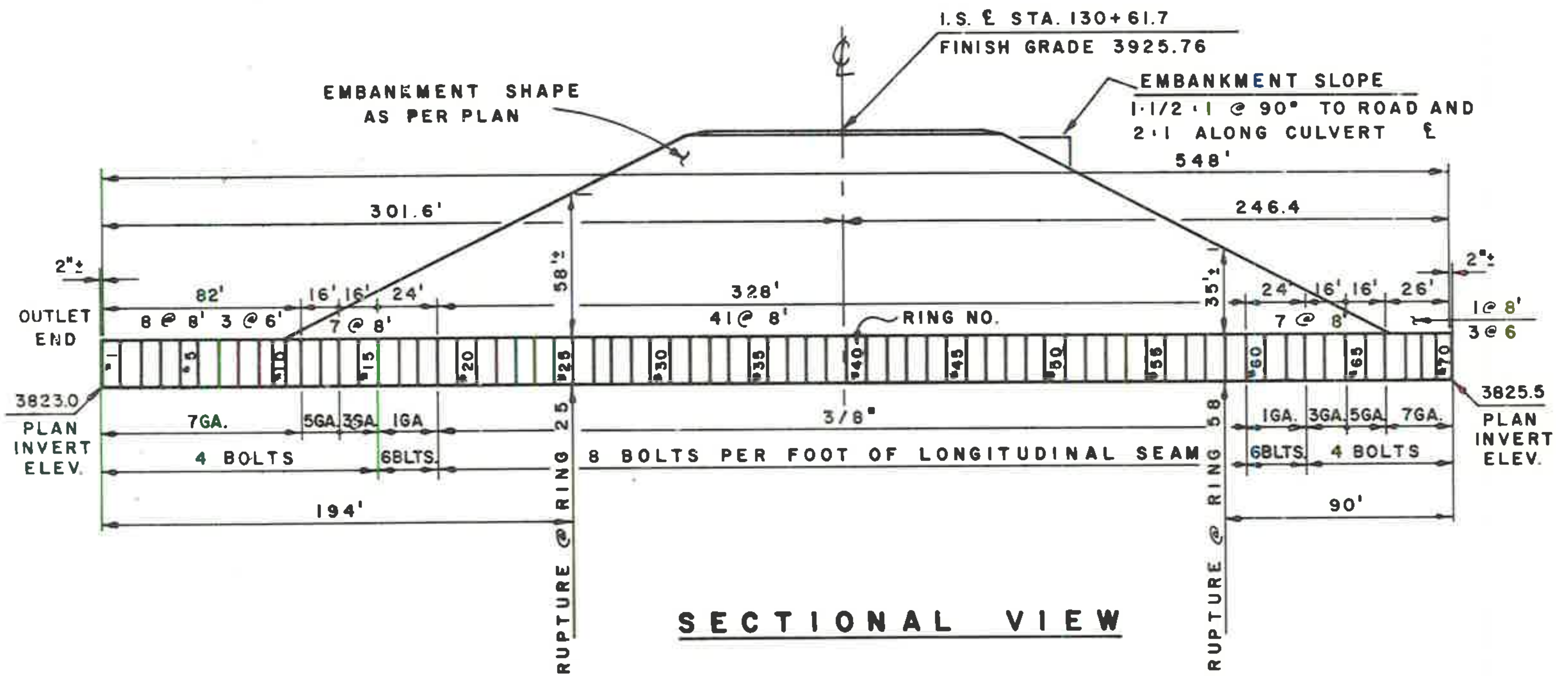


Figure 5. Section through culvert showing plate and bolting requirements.

did show that in laboratory tests their ultimate seam strength did exceed 270,000 lb per lineal ft. Copper-bearing steel was used for the tests and the pipe.

Other features of the ³/₈-in. thick plate, such as edge spacing and center to center distances of bolt holes, were the same as the standard for thinner gages. The corrugation spacing was the same as the standard with 6-in. pitch and 2-in. depth. However, due to the thickness of the plates, overlapping plates do not mesh as well as the thinner gages (Fig. 4). Since standard overlapping of plates in fabrication brings 3 plates together at corners, there is an unavoidable ³/₈-in. minimum width space at each corner, which permits water to enter or leave the pipe. All bolts and plates used in the pipe were galvanized. Plate lengths of 6 ft and 8 ft were used.

The culvert plates were stepped down from ³/₈-in. plates to 1 gage to 3 gage to 5 gage and to 7 gage in thickness at the ends of the pipe where the fill height was less, in order to reduce material cost (Fig. 5). Except for the central portion of the pipe where ³/₈-in. plate was used, 1-gage plate was used throughout the pipe in the invert to provide more erosion resistance than would be supplied by the lighter gages of pipe. The bolts used for all except the ³/₈-in. plates were ³/₄-in. ASTM A 325 bolts.

The special provisions stated that the pipe would not be strutted. It was considered unnecessary and undesirable and was not done during construction. An envelope of granular backfill material was called for to extend from 3 ft under, to 4 ft over the pipe and 12 ft wide on each side of the pipe (Fig. 6). The standard Montana Highway Department specification for backfill material was used, which consists of a granular material usually used for structure and culvert foundations and backfill. This allows a 4-in. maximum size gravel with at least 50 percent passing a No. 4 screen, or a sand, or a combination of sand and gravel. Ninety-five percent of maximum density was required for backfill material ranging from 100 to 120 lb per cu ft.

The special provisions required that the excavation and construction of the pipe be done under dry conditions, i.e., without standing or flowing water in the immediate construction area. The contractor had the option of diverting the stream through pipes, ditches, flumes, or by other means. He chose to use a timber flume. The granular backfill bedding was built up to a highly compacted flat surface upon which the pipe was fabricated. During construction of the pipe and the embankment above it, the contractor was required to maintain traffic through the area since there was no frontage road or other convenient bypass in the area. An impervious clay core completely surrounding the pipe was specified and constructed 42 ft downstream from the inlet.

A placement control device for checking culvert movement during backfill and embankment construction consisted of a plumb bob fastened to a bar hanger on the top inside of the pipe and a location reference assembly on the culvert invert. The latter consisted of a flat steel plate 2 ft sq on which was welded a 3-ft length of 15-in. diameter 14-gage corrugated metal pipe in a vertical position. This pipe was designed to offer protection from water and rocks to a ³/₄-in. diameter steel rod also mounted vertically inside the corrugated metal pipe. This rod provided a point reference for the suspended plumb bob. The whole reference assembly was secured to bolts fastened to the invert of the pipe. Fourteen of these assemblies were placed in the middle portion of the culvert at an average spacing of 30 ft apart. This provided a reference to check for rotation or unequal lateral deflection as well as vertical deflection.

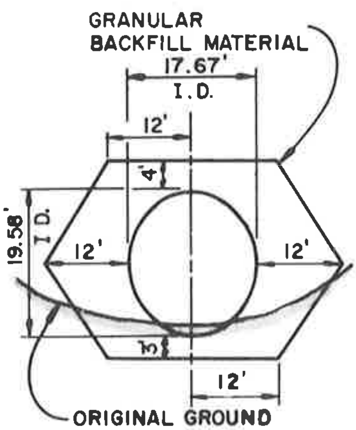

Figure 6. Section of envelope of select material that encased pipe.

Special provisions required that at the stage of construction when the embankment was to a height of 10 ft over the top of the pipe that the vertical dimension of the pipe was to be within plus 6 in. and

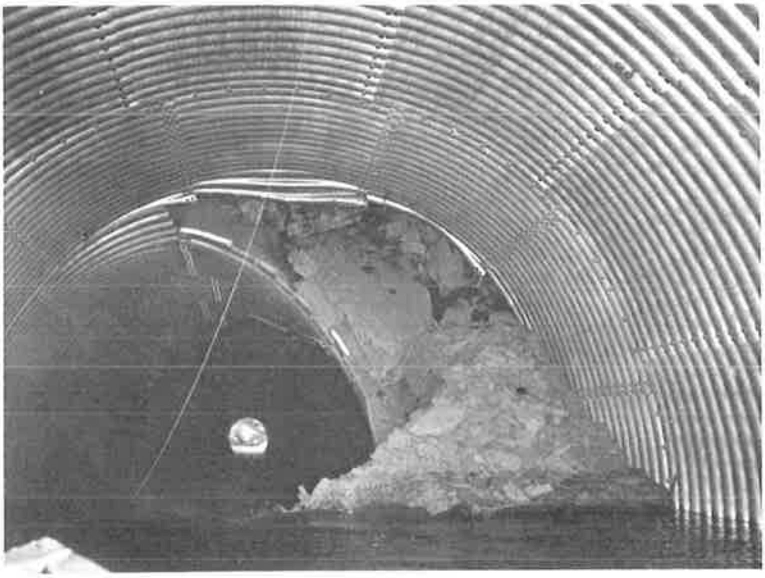

Figure 7. Looking downstream toward failure at ring 58.

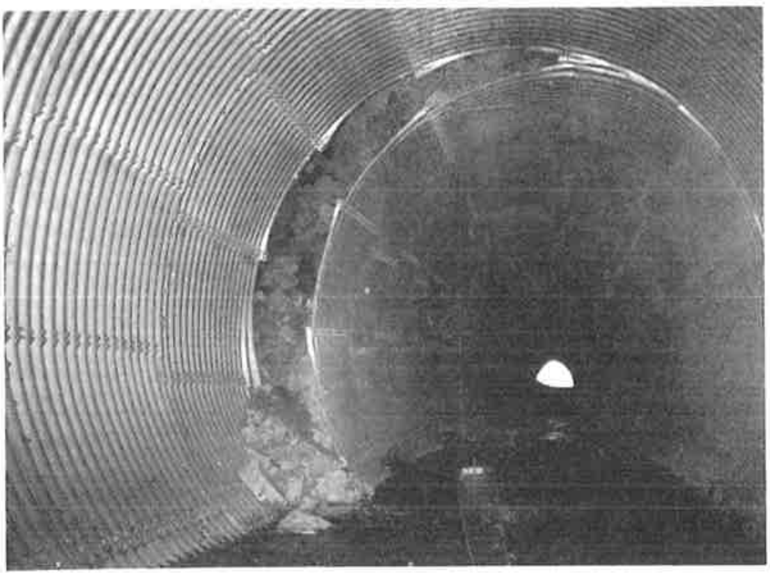

Figure 8. Looking upstream toward failure at ring 25.

minus zero inches of the 5 percent ellipsed shape detailed. Checking at this stage of completion revealed that this tolerance was met. No other deflection measurements were taken after this stage of completion was reached. No other form of deflection control, check, or instrumentation was specified or carried out on this project.


Figure 9. Failure of longitudinal seam allowed plate slippage.

## FAILURE OF THE CULVERT

The installation of the culvert began in November 1963, under the construction inspection of the Montana Highway Department. Roadway excavation and placement of embankment over the pipe continued at varying rates through the winter months. Full height of the embankment was reached in early spring of 1964. The second week of June 1964 brought heavy rains and high runoff from the continental divide in the northwestern part of Montana. There were many bridge, highway, and road washouts along with much building flooding in urban areas as a result of the floods. The Little Prickly Pear Creek also had high runoff at this time. However, it was less than the design highwater condition since the large culvert was flowing less than one-half full.

A rupture in the pipe wall was observed from outside the pipe and reported on July 13 by a bulldozer operator who was clearing the creek channel. Subsequent inspection inside of the pipe revealed that two major ruptures and displacements in the circumferential ring seams had occurred. The upstream one was 90 ft from the inlet and occured between the first and second rings of $^3/_8$-in. plate at this end. A lateral displacement of 5 ft had taken place on one side of the pipe at midheight. A large amount of embankment material moved into the pipe through this opening forming a dam 7 ft high inside the pipe causing water to back upstream from the inlet (Fig. 7). A small depression on the surface of the embankment slope was noticeable above this area. The depth of cover over this location was 35 ft. The downstream displacement of 2.4 ft was of the same type, except that a smaller amount of material moved into the pipe and was washed away (Fig. 8). There were 58 ft of fill above this rupture. It also occurred in the $^3/_8$-in. plate between the seventh

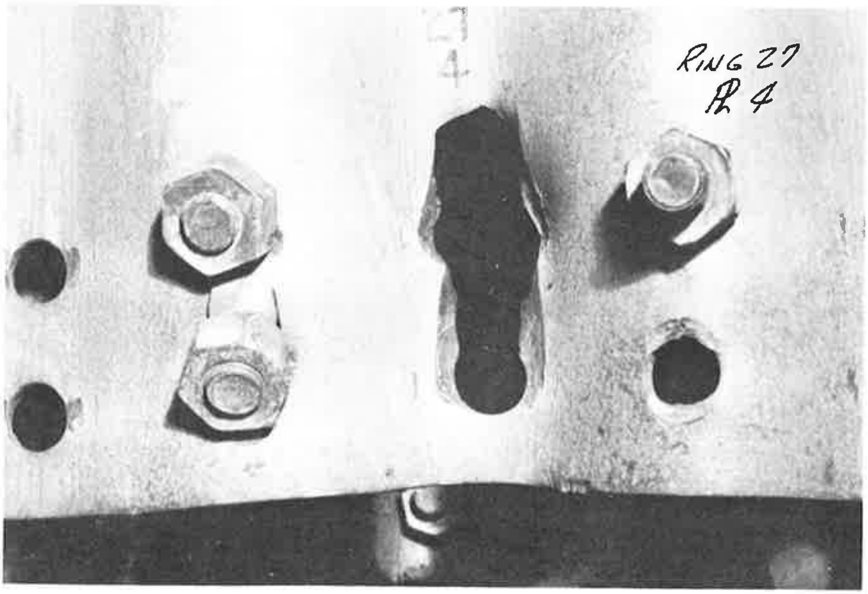


Figure 10. Evidence of plate galling at bolt holes.

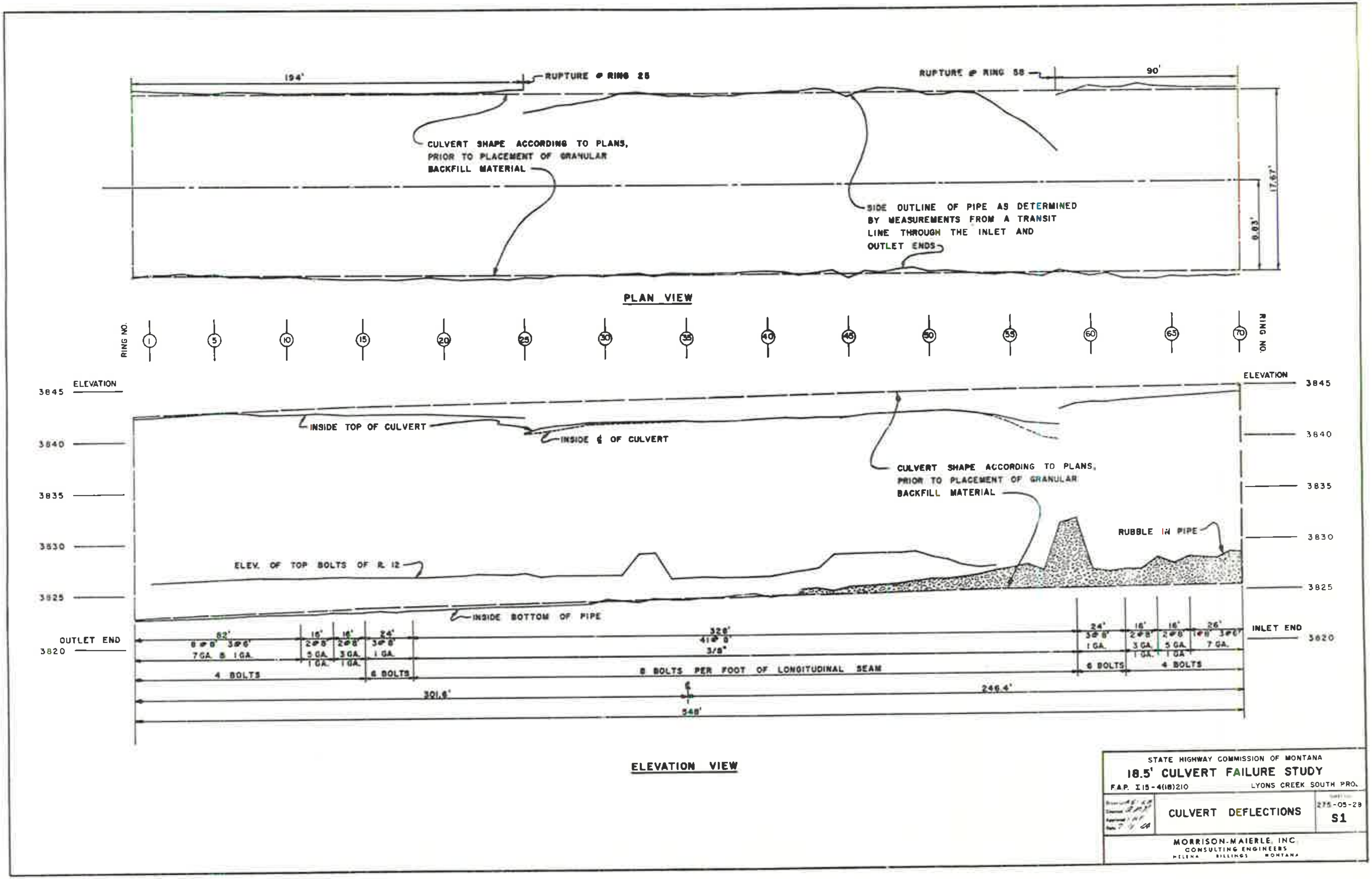


Figure 11. Deflections in pipe after rupture.

and eighth rings from the downstream end of the heaviest plates and 194 ft upstream from the outlet end.

Between the ruptures a longitudinal seam failure had occurred in each ring. The overlapping plates moved past each other 4 to 5 ft, producing a reduction in culvert diameter to 16 ft (Fig. 9). Bolts were sheared and missing not only in the longitudinal seams that had bypassed each other but in other seams that did not have a complete failure. The failure occurred only where the ASTM A 354 bolts were used, which was in all of the $^3/_8$-in. plates. The embankment material above the pipe arched and stabilized because the pipe with ruptured seams would have been incapable of supporting the load had this not occurred. There was no way of knowing how long prior to discovery of the rupture that the failure occurred and whether it was relatively instantaneous or over some period of time (Fig. 10).

A survey crew was immediately assigned to obtain measurements to determine the magnitude of movements. The results showed that the lowest invert elevations were not over a few tenths below the plan elevations of the pipe, which indicated very little settlement had occurred in the subgrade below the pipe. The alignment of the sides of the pipe in plan view showed that they had moved out of position very little except at the locations of the 2 major circumferential ruptures. Most of the extensive failure in the longitudinal joints occurred in the first 2 seams below midheight of the pipe and did not occur consistently on one side of the pipe (Fig. 11).

## RECONSTRUCTION OF THE CULVERT

From an evaluation of the available alternates for repair or replacement it was determined that the only feasible operation would be to uncover the pipe. This was done and reconstruction of the pipe has been completed. This included the replacement of damaged plates and replacement of all $^3/_4$-in. ASTM A 354 bolts with $^7/_8$-in. ASTM A 325 bolts. The granular backfill envelope around the pipe was replaced and the bed was shaped to fit the bottom of the pipe to the greatest extent possible. An imperfect trench effect was constructed with baled straw placed over the pipe from 5 ft to 7.5 ft above the pipe and for the full width of the pipe. It extends for almost the full length of the pipe. The embankment material above the baled straw was loosely placed for a height of 6 ft. The placement of embankment to full height was completed in January 1966, and traffic has been using it since then.

Various theories were advanced regarding the cause of the failure. These included penetration and washing of the granular backfill due to high water runoff, vibrations from rerouted trains due to flooded railroad tracks elsewhere, and a mass movement caused by an earthquake or slides in the area. Other more conventional construction factors have been questioned regarding their possible contribution to the failure. These include the magnitude of the adverse influence of using a flat bed instead of a shaped bed on which the culvert was placed, the backfilling and compaction procedures used, and culvert fabrication procedures such as bolt tightening. None of these factors has revealed a conclusive answer to the cause of the failure.

Extensive testing of ASTM A 354 bolts revealed that under a certain combination of environment conditions a phenomenon known as hydrogen embrittlement can occur, which results in reduced strength of the bolts (1). A paper covering this subject as it applies to the ASTM A 354 bolts and bolting procedures used on the Wolf Creek culvert project has been prepared by the Armco Steel Corporation and should be consulted for complete information.

A program to provide checking, testing and control of the culvert and embankment reconstruction has been conducted by the Engineering Department of Montana State University at Bozeman as a research project under the direction of the Montana Highway Department and with the cooperation of the Bureau of Public Roads. The checking and reading of SR 4 strain gages and Carlson soil stress meters used in the control program is expected to continue for some time in order to have the fullest evaluation of culvert stresses and the effectiveness of the imperfect trench used in the reconstruction.

## REFERENCE

1. Engineering News Record, Aug. 12, 1965, pp. 126 and 130.

# Research on Bolt Failures in Wolf Creek Structural Plate Pipe

JOHN N. MACADAM, Research Engineer, Research Center, Armco Steel Corporation, Middletown, Ohio

An investigation of high strength bolts in ⅜-in. thick structural plate was undertaken following discovery of an 18½-ft diameter pipe failure at Wolf Creek, Montana, in July 1964. Fractured A 490 bolts were found to meet ASTM hardness and chemistry requirements. Static load seam strength tests on ¾-in. diameter A 325 and A 490 bolts in ⅜-in. corrugated structural plate were made to determine effects of initial bolt torque, reduced temperatures, freezing water, and prying action from plate bending. No evidence of bolt or joint weakness was observed.

Further research and tests showed that A 490 bolts comparable to Wolf Creek bolts ($R_C$ 38) were susceptible to hydrogen embrittlement. Environmental conditions required for cathodic charging of atomic hydrogen were present in the Wolf Creek pipe. Sustained bolt stress levels above a threshold value apparently led to hydrogen-stress cracking. Hydrogen-stress cracking offers a logical explanation of the field failure.

•IN July 1964, joint failure of an 18½-ft diameter structural plate pipe on the Wolf Creek Canyon Interstate Highway in Montana was discovered. Several hundred bolts had broken in the structural plate seams allowing the plates to telescope circumferentially 4 to 5 ft in places.

This culvert structure is 548 ft long under a maximum rock fill height of 83 ft. In the center portion, where fill loads are greatest, ⅜-in. thick plates are used with ¾-in. ASTM A 490[1] high strength bolts. Near the ends lighter gage plates are used with ASTM A 325 bolts (Fig. 1).

The structure was erected and backfilled in November 1963. Construction of the embankment was temporarily halted in January 1964, due to winter weather conditions. Until then, alignment of the structure was checked using plumb bobs inside the pipe. Any failure up to that time would certainly have been noticed. Construction was resumed in the latter part of March and completed in April 1964. The failure was not discovered until early in July. It is possible that the structure was not observed for the 6-month period between January and July.

Standard practice is the use of ¾-in. A 325 high strength bolts in "Multi-Plate" structures. For ⅜-in. thick plate, however, ¾-in. A 490 bolts were used to provide an increase in the bolt shear capacity. Installation torques were stipulated to be 200 ft-lb minimum and 400 ft-lb maximum[2]. It is the opinion of several engineers who inspected the failed pipe that the stipulated maximum torque was exceeded. The degree of

Paper sponsored by Committee on Culverts and Culvert Pipe and presented at the 45th Annual Meeting.

[1]Formerly referred to by ASTM designation A 354 Grade BD; for ¾-in. diameter bolts the significant properties are identical.

[2]Application of high strength bolts in structural plate joints is not to be confused with use of high strength bolts in usual structural bearing or friction-type connections; such connections usually consist of lapped flat plate elements connected by means of bolts tightened to proof load initial tension.

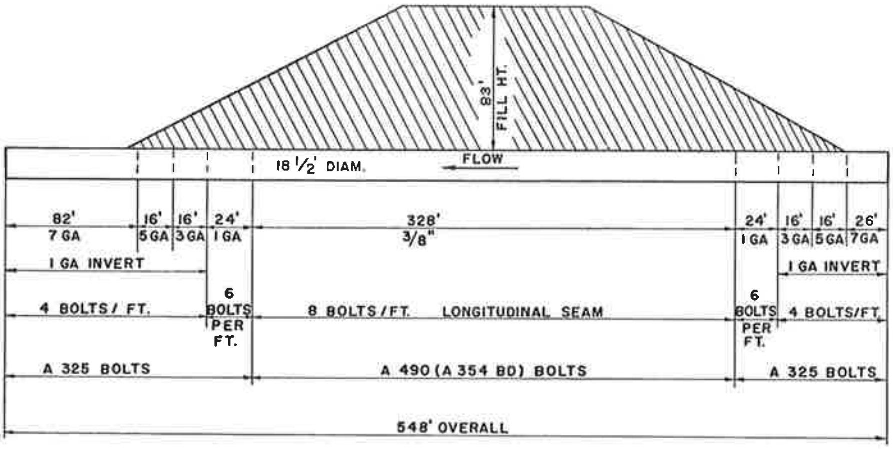


Figure 1. Wolf Creek structural plate pipe.

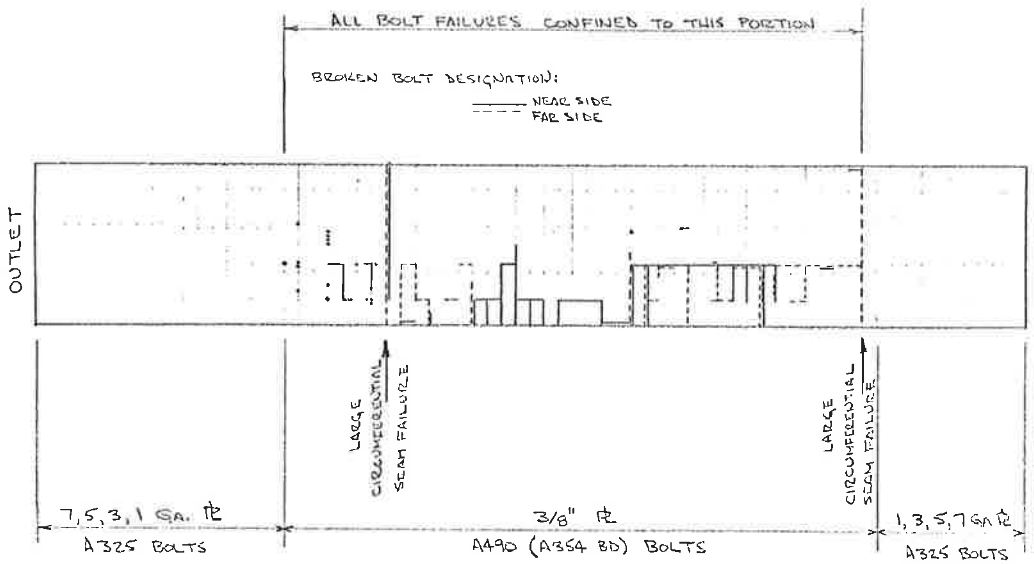


Figure 2. Diagram of failure.

nut disfiguration and the apparent "dimpled" effect at the bolt holes require torque in excess of 400 ft-lb.

All failed bolts were A 490 in $^3/_8$-in. plate. No failures occurred among the A 325 bolts used in the lighter gage plates. Beginning at the first ring of $^3/_8$-in. plate from the outlet end of the pipe, a few bolts were broken in the seams in the lower half of the pipe. No movement of the plates had occurred up to 194 ft from the outlet end, at which point there was a large circumferential seam failure. Another large circumferential seam separation occurred 90 ft from the inlet end of the pipe, which was one ring removed from the juncture of $^3/_8$-in. and 1-gage rings. Between these 2 circumferential failures, the plates in the lower half of the pipe had telescoped to within 1 to 2 ft of each other at longitudinal seams, reducing the pipe diameter to approximately 16 to 17 ft. These seams were boltless with the nut or head of bolt missing. Several other longitudinal and circumferential seams had failed bolts in this portion of the structure.

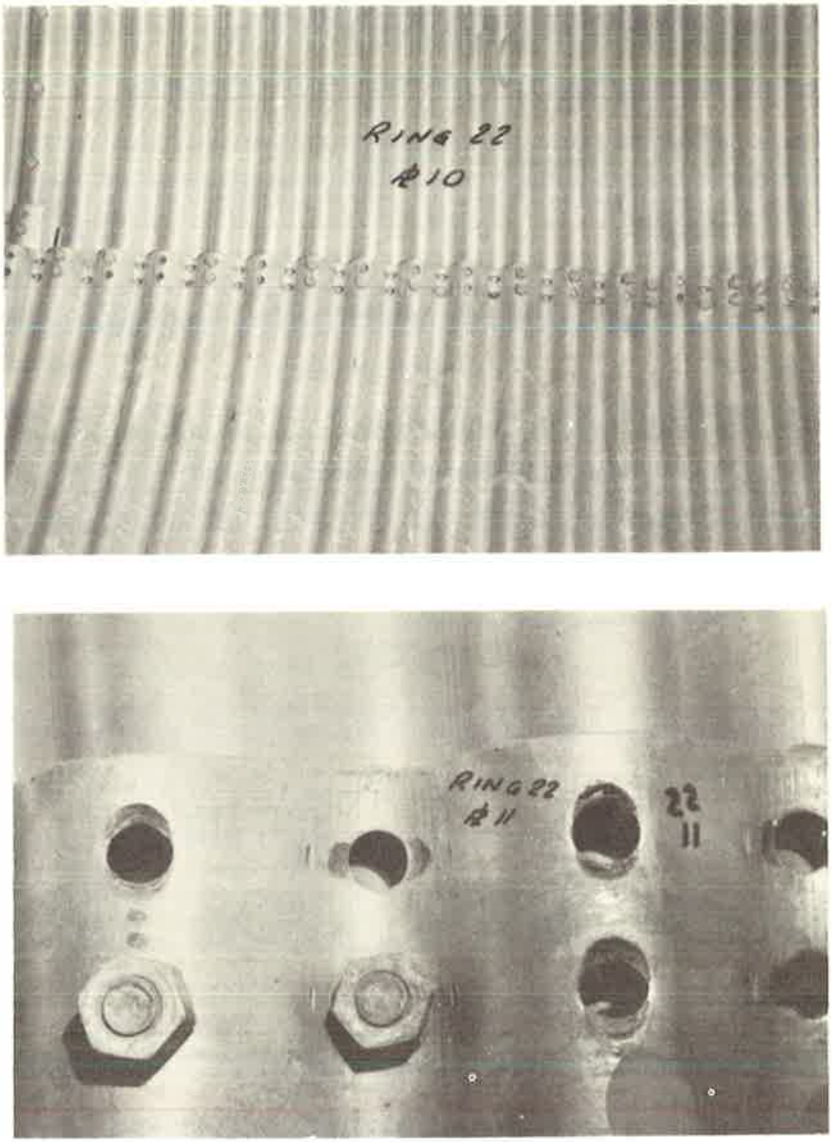


Figure 3. Longitudinal seam—no deformation of plate material at bolt holes.

Figure 2 is a diagram of the failure showing the location of broken bolts and the pattern of failure.

Engineers inspecting the failure reported that in most instances (except where circumferential seam bolts had obviously sheared to accommodate the change in shape of the failed structure) there was no evidence of any distortion of the plate at the bolt holes (Fig. 3).

After the failure had been discovered, it was quite difficult to assess the primary cause by visual observation of the structure. The failure was sufficiently catastrophic so that several types of failure were evident.

TABLE 1

BOLT PROPERTIES

**Hardness (Determined in accordance with ASTM A 370 Sec F4)**

| Bolts | Rockwell C Hardness Min | Rockwell C Hardness Max | ASTM Specs. Min | ASTM Specs. Max |
|---|---|---|---|---|
| 1 | 37.0 | 37.5 | 32 | 38 |
| 2 | 36.5 | 37.5 | | |
| 3 | 38 | 38.5 | | |
| 4 | 36.5 | 37 | | |
| 5 | 36.5 | 38.5 | | |
| 6 | 38 | | | |
| Bolts used in investigation | | | | |
| ¾ in. A 325 | 30 | 30.5 | 23 | 35 |
| ¾ in. A 490 | 34 | 38 | 32 | 38 |

**Chemistry (Check analysis)**

| Elements | Bolts Used in Investigation: Wolf Creek | ¾ in. A 490 | ASTM A 490 Spec. | ¾ in. A 325 | ASTM A 325 Spec. |
|---|---|---|---|---|---|
| Carbon | 0.48 | 0.47 | 0.28 to 0.55 | 0.34 | 0.27 min |
| Manganese | 0.88 | 0.93 | | 0.82 | 0.47 min |
| Phosphorus | 0.020 | 0.013 | 0.045 max | 0.013 | 0.048 max |
| Sulfur | 0.026 | 0.024 | 0.045 max | 0.021 | 0.058 max |
| Nickel | 0.19 | 0.15 | | | |
| Molybdenum | 0.19 | 0.13 | | | |
| Chromium | 0.93 | 0.91 | | | |

**Tensile Strength (Avg of 3 tests on full size bolts)**

| Bolts Used in Investigation | Tensile Strength (lb) | ASTM Spec. |
|---|---|---|
| ¾ in. A 490 | 57,400 | 50,100 min |
| ¾ in. A 325 | 45,600 | 40,100 min |

Figure 4. Broken bolts obtained from Wolf Creek.

## BOLT AND PLATE PROPERTIES

Approximately 40 broken bolts were obtained from Wolf Creek following discovery of the failure. Hardnesses determined on 6 Wolf Creek bolts are given in Table 1. Check analysis chemistry is also given. Hardness and chemistry meet ASTM requirements indicating that failure was not due to defective bolt material.

Generally, the fracture surface of the bolts was of a brittle nature. The fractures occurred in the threads at various distances from the nut. If bolt shear had been the mode of failure, the fracture surface would be along the shear plane, which is one plate thickness from the nut for lapped joints. Several of the fracture surfaces were rather flat and perpendicular to the axis of the bolt. This type of fracture could possibly be identified with torsion-tensile failure (Fig. 4).

For the purpose of investigating the behavior of high strength bolts in ⅜-in. thick structural plate, supplies of both A 325 and A 490 galvanized Armco "Multi-Plate" bolts were obtained. These bolts were manufactured in the same manner as those used

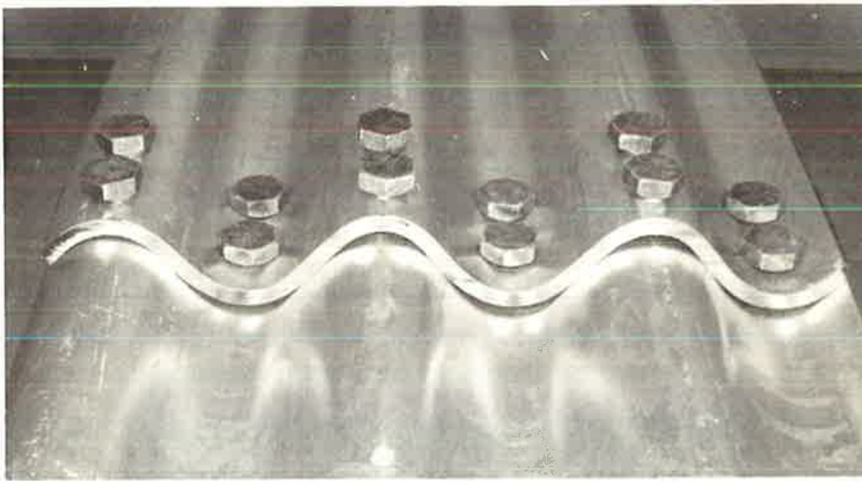

Figure 5. Fit between $^3/_8$-in. plates with bolts torqued to 200 ft-lb.

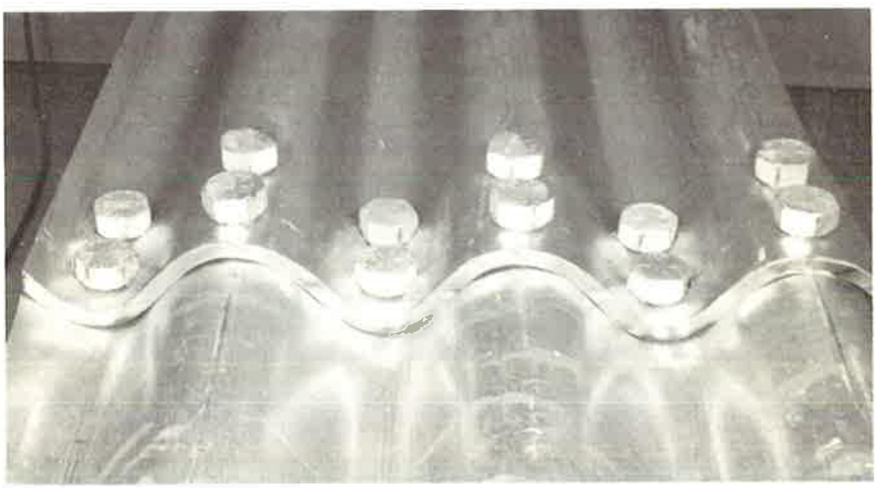

Figure 6. Fit between $^3/_8$-in. plates with bolts torqued to 910 ft-lb.

in the Wolf Creek pipe. ASTM A 325 is a quenched and tempered carbon steel bolt, and A 490 is a quenched and tempered alloy steel bolt. Properties of these bolts are also given in Table 1. Note that properties of the A 490 bolts acquired for the investigation are close to the actual Wolf Creek bolts.

Both grades of bolts were inserted in a joint of $^3/_8$-in. structural plate and torqued to failure to determine ultimate torque values. Average results from 2 tests using the galvanized nuts and bolts as received were: (a) A 490 ultimate torque = 950 ft-lb, and (b) A 325 ultimate torque = 840 ft-lb.

Structural plate material used in the investigation was standard 6- × 2-in. corrugation, $^3/_8$-in. thick, hot-dip galvanized, copper-bearing steel.

When structural plate sections are connected by the single lap joint, the corrugations do not nest in intimate contact. Inherent gaps between plates at crests and valleys of the corrugations will depend on the plate thickness. The greater the thickness, the greater the gap distance. Figure 5 illustrates the gaps present in $^3/_8$-in. thick plate with the bolts tightened to 200 ft-lb torque. A torque of approximately 800 ft-lb was required to essentially close the gaps in 6-in. wide joints. In a wide plate joint complete yielding of the cross section would be required to close the gaps. Figure 6 shows the fit between plates with A 490 bolts tightened to 910 ft-lb.

Any efforts in the field to draw the $^3/_8$-in. plates tightly together would require an excessive value of torque resulting in high initial bolt stress.

## SEAM STRENGTH TESTS

It has been stated that the bolt fractures appeared to be brittle. Temperatures inside the pipe could have conceivably fallen to the transition temperature of the bolt material. By this hypothesis, the high initial bolt stresses together with the notch effect from the threads might then result in a static brittle fracture of the bolts.

To investigate this possibility, bolted joints were assembled using both A 325 and A 490 bolts torqued to 89 percent of ultimate torque. These joints were lowered to -75 F in a dry ice bath. In one instance the A 490 assembly was subjected to approximately -320 F using liquid air. However, no bolt failures occurred either statically or by impact from a hammer blow.

It was then considered desirable to determine the effect of reduced temperatures on seam strength capacity. Another important factor related to the Wolf Creek failure needing study was the effect of high torques. Consequently, joint strength tests were made using A 325 and A 490 bolts with both initial bolt torque and temperature as variables.

Figures 7 and 8 show the type of specimen and test used to determine compressive seam strength. Testing facilities limited specimen width to 6 in. Four bolts were used corresponding to an 8-bolt-per-foot longitudinal seam. Three levels of torque and three levels of temperature were used in this experiment. Bolts were torqued to: (a) 200 ft-lb, which would be adequate for field installations; (b) torque corresponding to the tensile yield strength of the bolts; and (c) torque of at least 95 percent of the ultimate torque (Table 2).

Yield strength torques were determined by a calibration method using bolts with machined ends. These bolts were tightened to various levels of torque and measured before and after torque release. From these measurements of bolt length it was possible to establish the approximate point of nonlinear response, or permanent set, which was then taken as the yield strength torque.

All A 490 bolted joint compression specimens failed by plastic buckling and yielding of the plate material away from the bolted lap (Fig. 9). In some tests at reduced temperatures the "Multi-Plate" material cracked under high local stresses between the bolt holes (Fig. 10). A 325 bolted specimens failed in either of two modes—plate failure (Fig. 10) or bolt shear (Fig. 11).

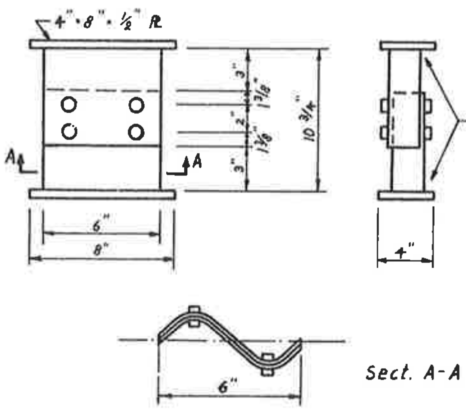

Figure 7. Joint strength compression test specimens.

No bolt shear failures were obtained in the laboratory tests on A 490 bolts. However, in the Wolf Creek pipe all broken bolts were A 490 bolts and none of the A 325 bolts failed. Several characteristics of the A 325 laboratory shear rupture surfaces worth noting are: (a) flowed metal across the bolt ruptures (Fig. 11) was plainly evident; (b) the rupture surface was consistently 10 to 15 deg from the perpendicular cross section of the bolts; and (c) threads of the bolt indented in the plate under bearing pressure. None of these effects were noticeable in the Wolf Creek failure, indicating that bolt shear was not the primary cause of the field failure.

Results of this experiment showed that the effect of initial tightening torque and

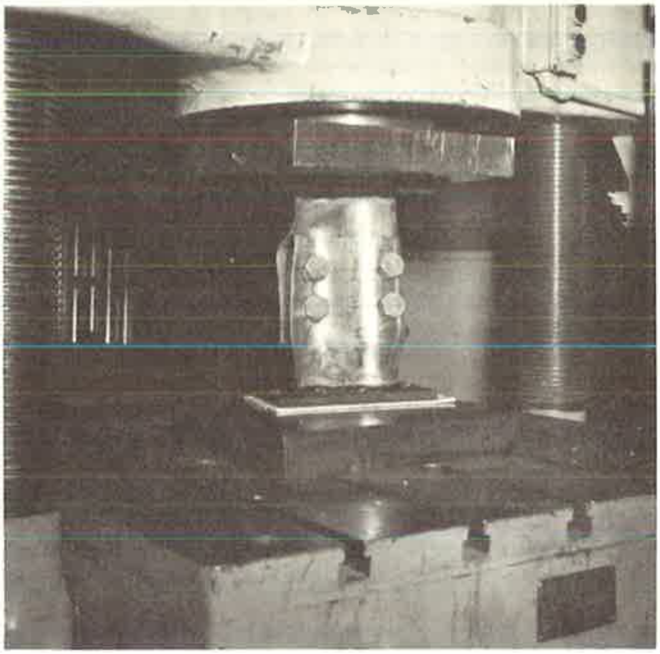

Figure 8. Joint strength test set-up.

TABLE 3

RESULTS OF JOINT STRENGTH TESTS

| A 325 Bolts[a] | | | | A 490 Bolts[a] | | | |
|---|---|---|---|---|---|---|---|
| Temp. (°F) | Torque, Ft-Lb 200 | 630 (75%) | 825 (98%) | Temp. (°F) | Torque, Ft-Lb 200 | 710 (75%) | 910 (96%) |
| Room Temp. | 122,200 lb—bolt shear, some plate failure | 128,900 lb—bolt shear, some plate failure | 121,500 lb—bolt shear, slight plate failure | Room Temp. | 120,000 lb—plate failure | 129,000 lb—plate failure | 130,600 lb—plate failure |
| -10 | 126,800 lb—plate failure, crack in plate | 129,800 lb—plate failure, crack in plate | Retorqued[c] to 825 ft-lb: 116,900 lb—same failure as above | -10 | 127,600 lb—plate failure | 131,800 lb—plate failure, crack in plate | Retorqued[c] to 910 ft-lb: 133,200 lb—same failure as above |
| -60 | 127,200 lb—plate failure, crack in plate | 128,500 lb—bolt shear, crack in plate, plate failure | 122,200 lb—bolt shear, crack in plate, slight plate failure | -60 | 129,800 lb—plate failure, crack in plate | 130,000 lb—plate failure, crack in plate | 135,500 lb—plate failure, crack in plate |

[a] ¾-in. bolts, 6-in. wide specimens with 4 bolts.

[b] Torque values shown in parentheses are percent of ultimate torque.

[c] Tests were run at room temperature after bolts retorqued to maximum value. Loss in torque of 80-86 percent.

specimen temperature on seam strength was of questionable significance. Wallaert and Fisher (1) have recently reported that initial bolt preload from tightening did not significantly affect the shear strength of A 490 bolts.

Bending moment applied to a lapped connection will cause tensile forces in the fasteners due to prying action, the magnitude depending on the rigidity of the connected parts. Structural plate in ⅝-in. thickness might conceivably provide sufficient rigidity to "pry" the bolts to tensile failure.

This possible explanation of the Wolf Creek failure was investigated by making beam tests on bolted structural plate joints. Forty-nine specimens, 1 in. long by 18 in. wide, were prepared with the bolted joint located at mid-span. The following 4 tests were made:

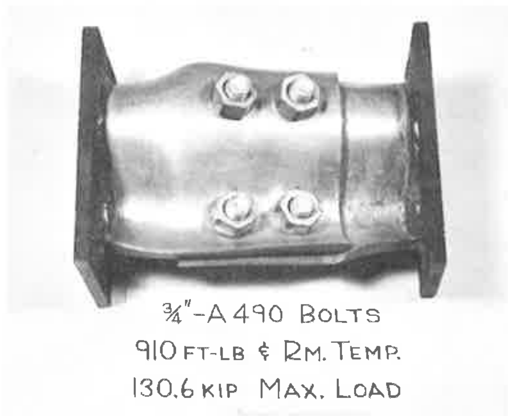


Figure 9. Typical plate failure.

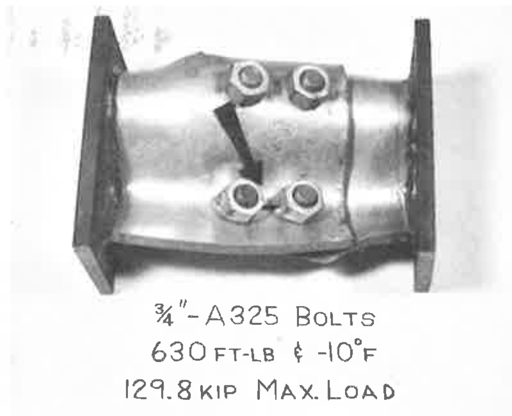


Figure 10. Typical plate failure with crack in plate between bolt holes in lower row.

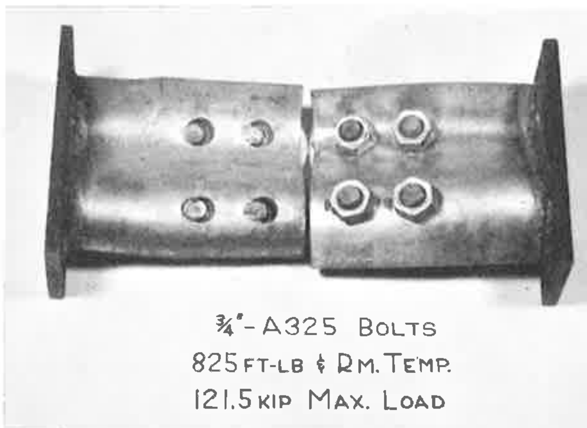


Figure 11. Typical bolt shear failure of A 325 bolts.

¾-in. - A 490 bolts at 200 ft-lb,
¾-in. - A 490 bolts at 910 ft-lb,
¾-in. - A 325 bolts at 200 ft-lb, and
¾-in. - A 325 bolts at 825 ft-lb.

Third-point loads were applied with an overall span of 45 in. (Fig. 12 and Table 3).

Ultimate loads were governed by plastic bending of the structural plate along a cross section at a row of bolts without any bolt tensile failures. The bending strength or rigidity of the ⅜-in. plate was lower than that required to cause prying forces equal to the tensile strength of the bolts. A typical beam test specimen after testing is shown in Figure 13.

An opinion was made that water freezing inside the lapped joints might create pressure sufficient to cause tensile failure of the bolts. It is true that most of the failed bolts were near or below water. To check this hypothesis, joint specimens were prepared such that water could be held between the plates. The freezing action did not fail the bolts.

The data show that the A 490 bolts were not mechanically defective as manufactured, and that the bolt failures could not be explained on any basis of mechanical weaknesses.

TABLE 3

BEAM TEST RESULTS

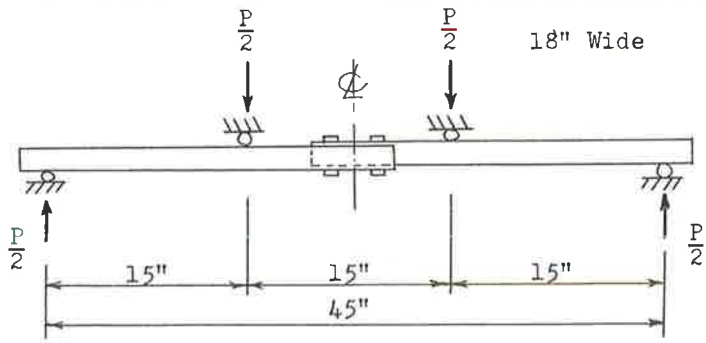


| Test No. | Bolts | Torque, ft-lb | Maximum Load, P (lb) | Equiv. Moment, in.-kip/ft | Failure Mode |
|---|---|---|---|---|---|
| 1 | A 490 | 200 | 26,250 | 131 | Plate plastic bending |
| 2 | A 490 | 910 | 30,100 | 150 | |
| 3 | A 325 | 200 | 28,100 | 141 | |
| 4 | A 325 | 825 | 30,000 | 150 | |

Note: Avg maximum moment = 143 in.-kip per ft of plate

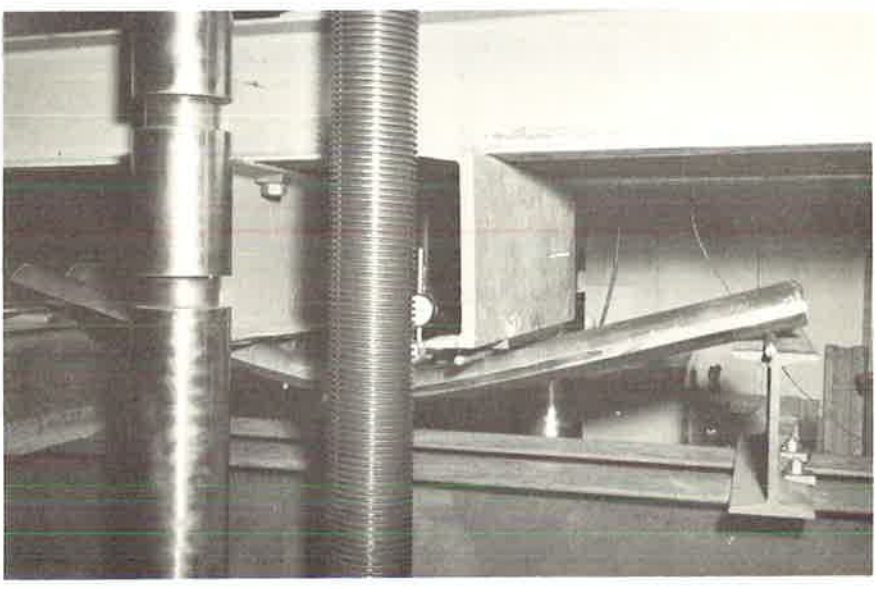

Figure 12. Beam test set-up. Bolted splice is behind screw column.

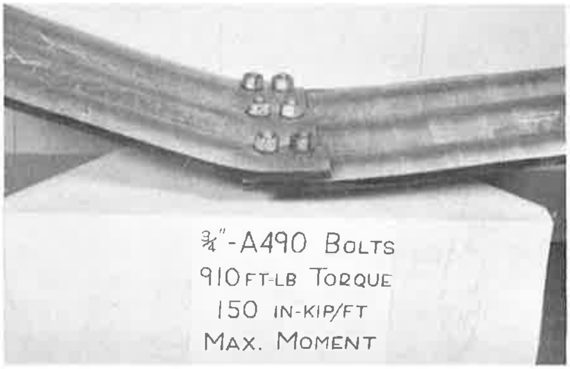


Figure 13. Typical beam test specimen after testing showing plastic bending failure of plate material.

Because the failures (Fig. 2) were near or below the water level, it appeared that an environmental effect such as corrosion might be the primary cause of failure.

## ASPECTS OF HYDROGEN EMBRITTLEMENT

If a steel is sufficiently hard and if it absorbs more than some minimum amount of atomic hydrogen, a sustained tensile stress may, in time, cause a crack leading to fracture. Moreover, the applied stress may be much lower than that required to cause fracture in the absence of hydrogen. Such failures are known to occur with very little ductility even though in a tension test the material exhibits normal ductility (2). These delayed, brittle failures can occur in all types of high strength steels except possibly those of strictly austenitic microstructure, although even this exception remains a matter of conjecture.

Although hydrogen embrittlement and hydrogen-stress cracking have been known and studied for many years (3), the mechanisms are still debatable. Actually, there is not yet a precise distinction between hydrogen embrittlement and stress-corrosion cracking in high strength steels. All of the theories advanced to explain the effects depend on a critical combination of hydrogen and stress (4).

Atomic hydrogen can be absorbed by the steel from cleaning (pickling) operations, plating operations, cathodic protection (5), or corrosion processes (6, 7). Extremely small amounts of hydrogen in conjunction with sufficient stress levels have been shown capable of causing delayed fracture (7). Under most conditions, the strength or hardness level of high strength steel under tensile stress is one important material factor affecting hydrogen embrittlement susceptibility. Alloy composition is a relatively unimportant factor (4). The susceptibility diminishes with decreasing strength or hardness and also diminishes with decreasing applied stress. For a given hardness level, time-to-fracture curves become asymptotic at an applied stress referred to as a threshold stress. No clearly delineated threshold stress has been established (3). However, numerous investigators have verified the concept that the minimum or threshold stress for hydrogen-stress cracking decreases for increasing tensile strength or hardness levels.

In many electrochemical cells hydrogen evolves at the cathode. Holidays or coating defects in high strength steel parts coated with zinc, cadmium, aluminum, etc., in the presence of an electrolyte are enough to set up an electrochemical cell. The exposed steel becomes the cathode. Atomic hydrogen so produced may readily enter the steel, and if it is under sufficient sustained tensile stress, delayed hydrogen embrittlement fracture may occur. Impregnating the steel with atomic hydrogen is sometimes referred to as "cathodic charging."

Conditions necessary for cathodic charging were present in the Wolf Creek structure. The structural plates and bolts were hot-dip galvanized. Prior to galvanizing, the bolts

TABLE 4

CHEMICAL ANALYSIS OF LITTLE PRICKLY CREEK WATER DETERMINED BY MONTANA STATE BOARD OF HEALTH[a]

| Property | Content (ppm) |
|---|---|
| Total hardness (as $CaCO_3$) | 200 |
| pH | 8.2 |
| $CO_2$ | trace |
| Dissolved oxygen (at 45 F) | 11.4 |
| $H_2S$ | none |
| Total dissolved solids | 200 |
| Chloride (Cl) | 10 |
| Sulphate radical ($SO_4$) | 14 |
| Nitrates ($NO_3$) | none |
| Carbonate radical ($CO_3$) | 3 |
| Bicarbonate radical ($HCO_3$) | 217 |
| Total alkalinity ($CaCO_3$) | 183 |
| (1) Methyl Orange test | 5 |
| (2) Phenolphthalein test | 178 |
| Calcium (Ca) | 40 |
| Magnesium (Mg) | 24 |
| Iron (Fe) | 0.16 |
| Sodium and potassium calc. (Na-K) | 8 |
| Fluoride (F) | 0.7 |

[a]Little Prickly Creek is the stream that runs through the pipe, Wolf Creek is the name of the town nearby, and Lyons Creek South refers to the highway project. Sample taken 11/4/65, analysis reported 11/5/65.

were pickled in the standard practice of manufacture. It has been stated that pickling is a potential source of hydrogen embrittlement. However, this explanation does not appear to be valid in this case because of the pattern of failures being below probable water levels.

It is reasonable to assume that the zinc coating on the bolt threads was damaged during installation enough to expose some bare steel. Water flowing in and permeating the soil around the culvert could serve as the electrolyte. The stream water analysis is given in Table 4. This analysis undoubtedly varies throughout the year depending on the amount of rainfall and melting snow.

Exploratory tests were made to determine the hydrogen-stress cracking susceptibility of the A 325 bolts at $R_C$ 30 hardness and the A 490 bolts at $R_C$ 38 hardness. Bolts were loaded as short cantilever beams in bending by using the fixture shown in Figure 14. A small magnesium disk was used as the anode. This was done in an attempt to produce failures—if they would occur—in a reasonable length of time. It took 2 to 8 months in the field. This was too long for a lab test. The high hardness ($R_C$ 38) bolt assembly shown in Figure 14 was placed in a 3 to 4 percent salt solution and cracked as seen overnight. In a similar test a softer ($R_C$ 30) bolt did not crack after 92 hr.

Loading a bolt in tensile and torsional shear stresses by tightening the nut provides a better representation of actual application. To this end bolts were tightened in a sleeve-type block with windows in its sides for observing cracks (Fig. 15). Magnesium bars were connected to the block and then the complete assembly was placed in tap water. A high hardness ($R_C$ 38) bolt tightened to approximately 80 percent of the

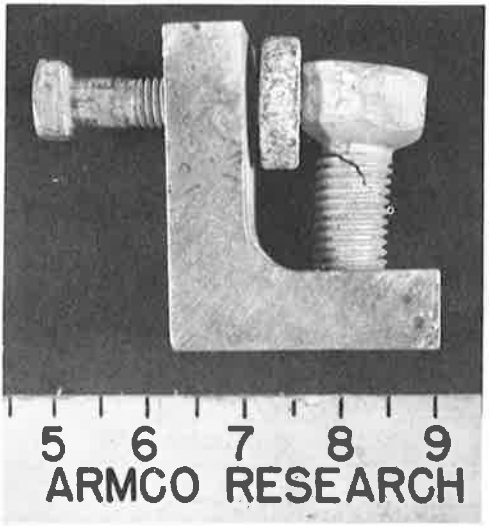


Figure 14. Preliminary test fixture used to determine hydrogen embrittlement cracking susceptibility of "Multi-Plate" bolts.

ultimate torque cracked after 4 days (Fig. 15). A softer bolt ($R_C$ 30) tested in the same manner had not cracked after 70 days. Numerous other tests on the low and high hardness bolts were made with attempts to vary the magnitude of stress, the electrolyte, and the method of charging. The same trend of results was obtained; i.e., the high hardness A 490 bolts (approximately $R_C$ 38) showed much greater susceptibility to hydrogen-stress cracking than the softer A 325 bolts (approximately $R_C$ 30).

These exploratory tests suggested that bolts at a hardness level comparable to the Wolf Creek bolts could be susceptible to hydrogen embrittlement. No evidences of bolt or joint weaknesses were observed in the static strength tests previously described. Therefore, a hydrogen-stress cracking hypothesis is offered as an explanation for the field failure. Field conditions tending to substantiate this hypothesis are:

1. The failure was of a delayed type since the bolts fractured sometime between January and July.
2. Failed bolts were predominately near and below the assumed water level in the pipe where a corrosion process could have occurred (Fig. 2).
3. Only the A 490 bolts failed. These bolts had the maximum hardness of the permissible range—$R_C$ 38. No failures occurred in the softer A 325 bolts.

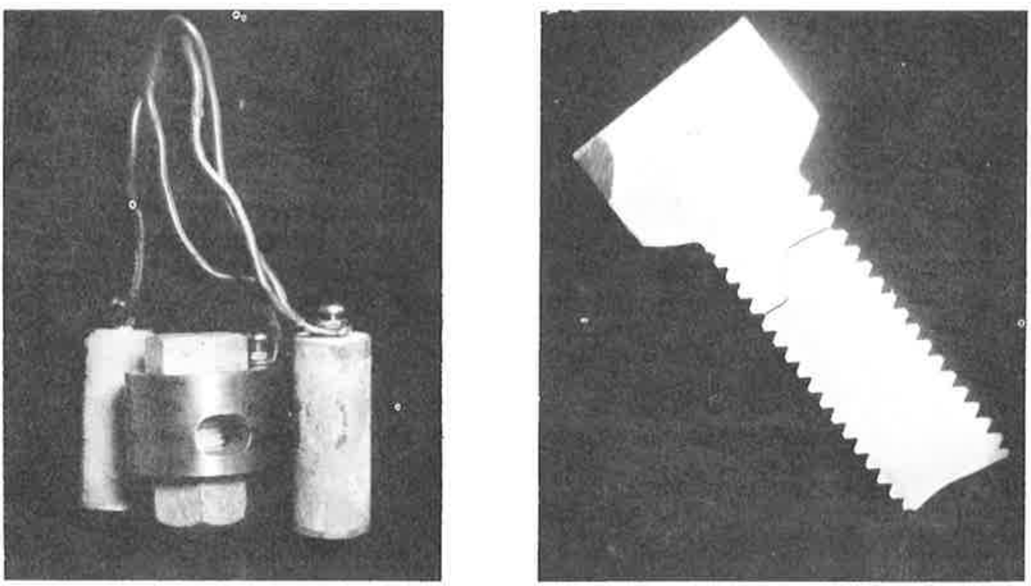

Figure 15. Bolt stressed by tightening in "solid" block: at right, cracks in $R_C$ 38 (A 490) bolt after 4 days in tap water.

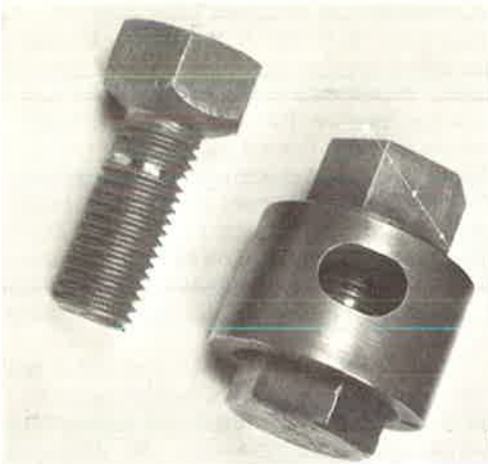

Figure 16. Machined bolt specimen and test block assembly for hydrogen-stress cracking experiments.

4. Tensile stresses were highest in the A 490 bolts as they were used exclusively in the ⅜-in. plates where greater torques were required to pull the plates together. A 325 bolts were used only in the lighter gage—1, 3, 5, and 7 plates.

5. The structure and bolts were galvanized.

6. Fractured bolts generally appeared to be brittle tensile failures.

7. There were instances of a few broken bolts in longitudinal seams which had not been displaced. These failures indicated that something besides shear weakness led to fracture.

Following the preliminary tests, hydrogen-stress cracking experiments were made under more controlled conditions, with different levels of sustained tensile stress on A 490 bolts. To determine the effect of hardness, a group of A 490 bolts was heat-treated to approximately $R_C$ 25. An annular groove was machined and polished to a depth slightly below the normal root diameter. This groove controlled the location of the hydrogen induced crack (Fig. 16). Bolts were tightened in the test block to desired tensile stresses by using the calibrated torque-tension relationship discussed later. The assembly was coated with wax leaving an exposed portion of the groove for hydrogen entry at each window opening in the test block. Specimens were placed in a 5 percent sulfuric acid solution containing approximately 0.05 percent sodium arsenite. A direct current of 1.5 to 2.5 amperes was maintained between the specimen and a Duriron bar anode (Fig. 17). At 15-min intervals the specimens were removed and examined under magnification for cracks (Table 5).

Time-to-fracture or first crack is used as a measure of hydrogen embrittlement susceptibility. Figure 18 shows time to crack and applied stress for both hardness levels. These data are in reasonable agreement with other investigations (5).

The threshold stress for $R_C$ 38 bolts was found to be approximately 20,000 psi, while the value for $R_C$ 25 bolts was approximately 48,000 psi. Actual cathodic charging

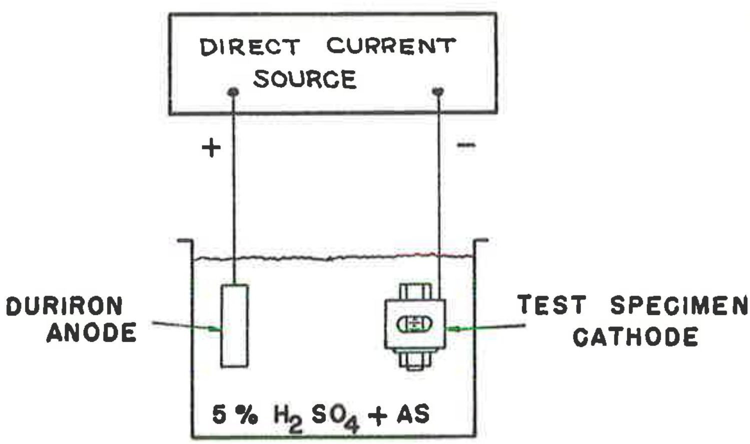


Figure 17. Hydrogen test method.

## TABLE 5

### RESULTS OF HYDROGEN-STRESS CRACKING TESTS UNDER CONTROLLED TENSION

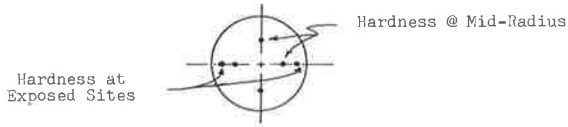


| Bolt No. | Applied Torque, ft-lb | Average Tensile Stress, psi | Hardness at Exposed Sites, $R_C$ | Hardness at Mid-Radius, $R_C$ Min | Max | Time to First Crack |
|---|---|---|---|---|---|---|
| 25-5 | 115 | 48,000 | 26-27 | 27 | 28.5 | no cracks (23 hr) |
| 25-6 | 115 | 48,000 | 25-24.5 | 24 | 24.5 | no cracks (24 hr) |
| 25-7 | 115 | 48,000 | 25-27 | 22.5 | 26.5 | no cracks (29 hr) |
| 25-2 | 170 | 68,000 | 24-24 | 24 | 25 | 210 min |
| 25-3 | 170 | 68,000 | 27.5-24 | 26.5 | 27.5 | 75 min |
| 25-4 | 170 | 68,000 | 25.5-25 | 24.5 | 26.5 | 120 min |
| 25-8 | 170 | 68,000 | 29.5-20.5 | 28 | 30 | 105 min |
| 38-11 | 40 | 20,000 | 38-38 | 38 | 38.5 | no cracks (23 hr) |
| 38-16 | 40 | 20,000 | 37-40 | 38.5 | 39 | no cracks (24 hr) |
| 38-17 | 40 | 20,000 | 39.5-40 | 39 | 39 | no cracks (24 hr) |
| 38-12 | 80 | 34,000 | 38.5-39 | 37 | 39.5 | 30 min |
| 38-4 | 115 | 48,000 | 38-37 | 37 | 38 | 90 min |
| 38-9 | 115 | 48,000 | 38.5-39 | 38 | 39 | 15 min |
| 38-10 | 115 | 48,000 | 39.5-39.5 | 39 | 40 | 45 min |
| 38-14 | 115 | 48,000 | 39-40 | 39 | 40.5 | 15 min |
| 38-15 | 115 | 48,000 | 39.5-39.5 | 39 | 40.5 | 15 min |
| 38-3 | 170 | 68,000 | 37.5-39 | 38 | 38.5 | 30 min |
| 38-6 | 170 | 68,000 | 39-38.5 | 39 | 39 | 30 min |
| 38-13 | 170 | 68,000 | 39.5-40 | 39 | 39.5 | 15 min |
| 38-19 | 170 | 68,000 | 38-39 | 37.5 | 38 | 15 min |
| 38-2 | 250 | 97,000 | 38-38 | 37 | 38.5 | 15 min |
| 38-5 | 250 | 97,000 | 39-38.5 | 39 | 40 | 15 min |
| 38-7 | 250 | 97,000 | 39-39 | 39.5 | 40.5 | 45 min |
| 38-18 | 250 | 97,000 | 39-40 | 39 | 40 | 15 min |

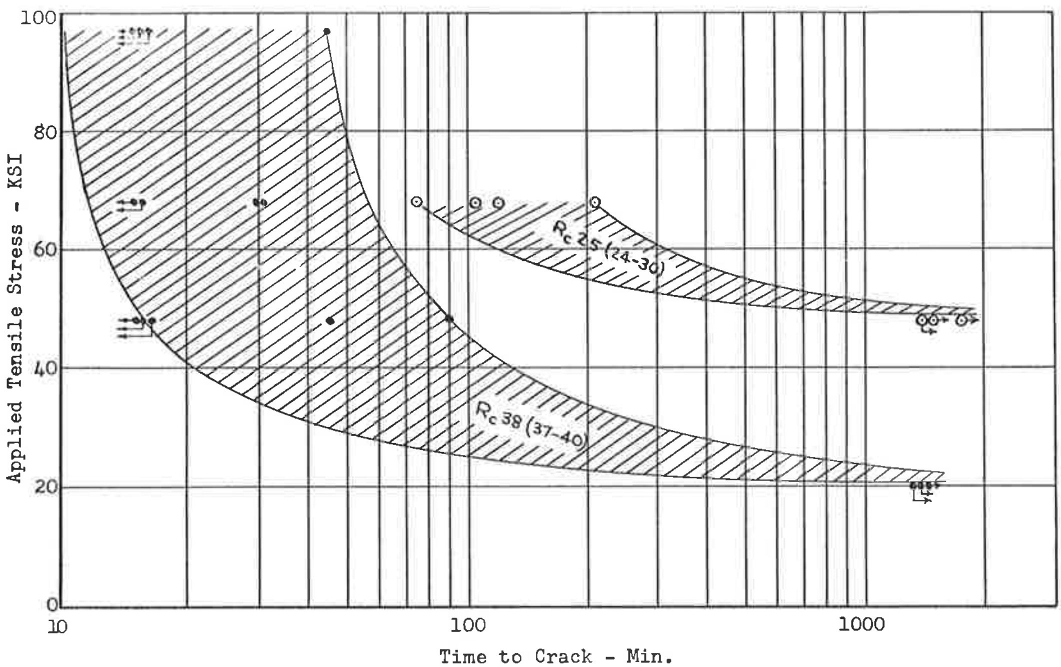


Figure 18. Hydrogen-stress cracking experiments.

conditions expected in the field would, of course, be much less severe. The time factor associated with hydrogen-stress cracking in the field would be much greater.

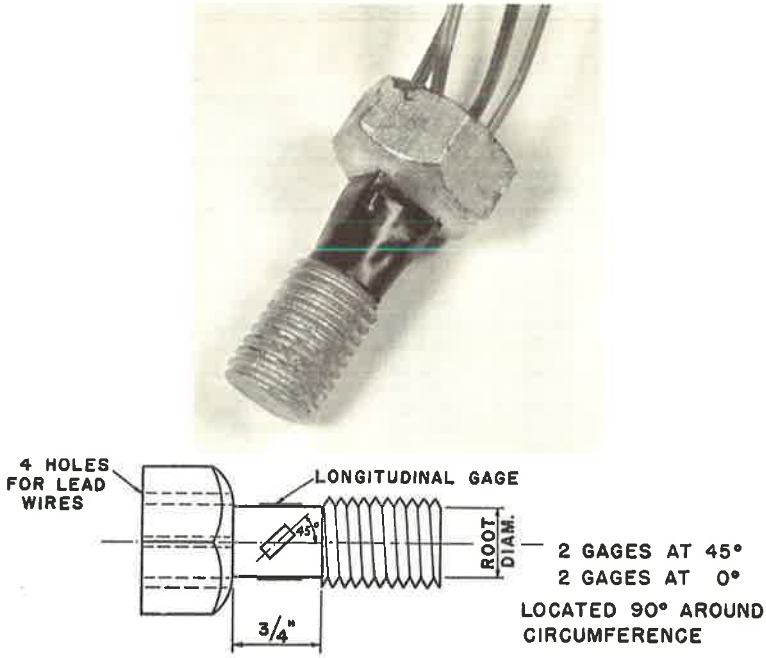


Figure 19. Strain gage instrumented bolts.

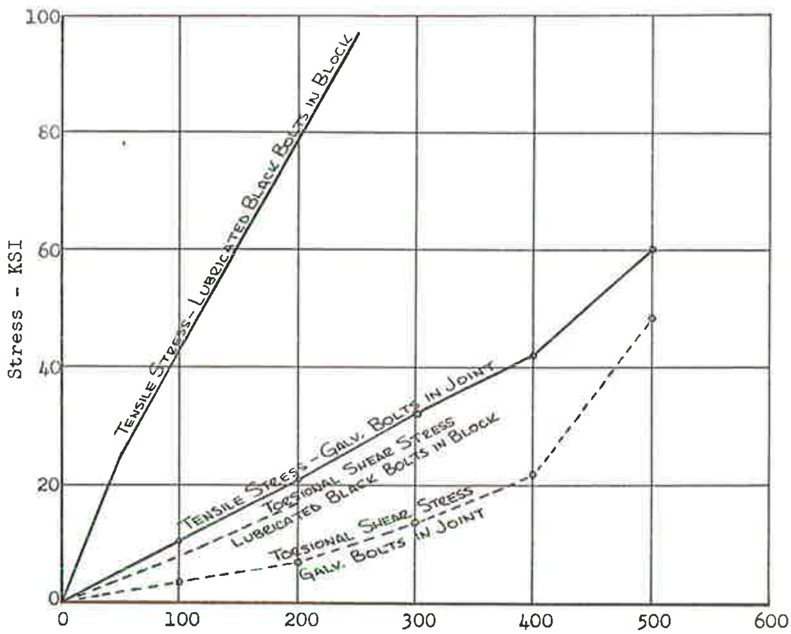


Figure 20. Comparison of bolt stresses vs torque.

## BOLT STRESSES RELATED TO APPLIED TORQUE

In usual structural joints using high strength bolts for friction-type or bearing-type connections, the bolts are installed by either the calibrated wrench method or the turn-of-nut method (8). Present-day specifications and practice no longer refer to torque values for installing bolts to minimum bolt tension values[3]. The commonly used turn-of-nut method involves certain nut rotations from a condition of connected parts being in full contact with each other ("snug tight"). This procedure is therefore not applicable to structural plate joints since the corrugations are inherently un-nestable. The concepts of bolting heavy structural joints are not applicable to structural plate pipe joints.

For this investigation it was desirable to ascertain the tensile and torsional shear stresses in the structural plate bolts as related to applied torque. Stresses were determined from strain gage instrumented bolts (Fig. 19). From this gage arrangement it is possible to determine tensile and torsional stresses for elastic conditions. Formulas for computing tensile stresses and torsional shear stresses are given in the Appendix.

One series of tests was made on instrumented bolts in the galvanized condition tightened in a galvanized structural plate joint. The stress-torque relationship is shown in Figure 20. Note that the torsional shear stress begins to increase significantly for applied torques above approximately 400 ft-lb. For increasing values of torque, torsional shear stress increases due to increasing friction developed by: (a) galling of the zinc at the thread contact surfaces, and (b) wedging action of the spherical seated nut into the hole in the plate.

Similar tests were made to calibrate tensile stress values for the hydrogen-stress cracking experiments. It was necessary to provide for a consistent torque-tension relationship for the hydrogen tests. To accomplish this the zinc was removed from the bolts, special nuts were made and hardened to give a better fit between bolt and nut threads, and the threads were lubricated. Bolts were tightened in the hydrogen test block (Fig. 16). Lubricant was applied to the contact surfaces between nut and block (Fig. 20).

The black bolts with lubricated threads and hardened nuts tightened in the "solid" block are stressed predominately in tension, while the torque applied to galvanized nuts and bolts in a galvanized structural plate joint results in high torsional shear stresses (Fig. 20).

## SUMMARY

This investigation of high strength bolts in ⅜-in. thick structural plate was undertaken following discovery of the Wolf Creek, Montana, pipe failure in July 1964. The Wolf Creek structure is an 18½-ft diameter pipe culvert installation under an 83-ft high fill. Several hundred A 490 (A 354 BD) bolts were found broken in the longitudinal and circumferential seams in the ⅜-in. plate portion of the culvert. Failed bolts were predominately located in the lower half of the pipe. In 40 percent of the culvert structure, near the ends, lighter gage plates were connected with the normally-used A 325 bolts. No bolt failures occurred in these portions of the culvert. Failed bolts obtained from the Wolf Creek pipe were found to meet ASTM Designation A 490 hardness and chemistry requirements.

In an effort to analyze and resolve the failure, seam strength tests were made using both ¾-in. A 325 and A 490 bolts in ⅜-in. structural plate joints. It is known that bolts in the field structure were installed in many instances with excessively high values of torque. To check influence of high torques and low temperatures, joint-strength tests were made with bolts torqued to 95 percent of breaking torque and at reduced temperatures to -60 F. These tests showed that high initial torques and/or low temperatures had negligible effect on joint strength.

The laboratory static load test failure mode for ⅜-in. plate with ¾-in. A 490 bolts (8-bolt-per-foot seam) is plate buckling and yielding, not bolt shear. Observations of

---

[3] In usual structural connections, bolts are tightened to a tension at least equal to the bolt proof load.

the field failures indicated that bolt shear was not the primary mode of failure, although several modes of failure were evident in the final catastrophic state of the culvert pipe.

Since many of the failed bolts appeared to be tensile-type fractures with little ductility, the possibility of tensile failure from prying action during bending was investigated. However, bending moment applied to the joints in beam tests resulted in plastic bending of the structural plate with no bolt tensile failures from prying action.

No evidence of bolt or joint weakness was observed in any of the static strength tests made in the laboratory in search of a plausible explanation of field failure.

Laboratory tests revealed a high degree of susceptibility of A 490 bolts at $R_C$ 38 hardness to brittle fracture when cathodically charged. Cathodic charging of atomic hydrogen could have occurred in the Wolf Creek pipe because (a) the structure was galvanized; (b) installing bolts can result in damaged coating on the threads leaving exposed steel to be cathodic in the electrochemical cell; and (c) water was present to serve as an electrolyte. As a result of over-torqueing, the bolts probably were under sustained stress that was greater than a threshold value necessary for hydrogen-stress cracking.

Only high hardness A 490 bolts generally located below water failed. It was a delayed-type failure occurring in a period between 2 and 8 months after erection. The fracture surfaces of broken bolts appeared to be brittle tensile failures. These points provide circumstantial evidence tending to support a corrosion induced hydrogen-stress cracking hypothesis. This hypothesis offers a logical explanation of the field failure. Its mechanism more closely matches the observed field conditions than do mechanisms attributable to simple bolt weakness or to general overload of the structure.

## REFERENCES

1. Wallaert, J. J., and Fisher, J. W. Shear Strength of High Strength Bolts. Jour. of Struct. Div., ASCE Proc., Vol. 91, No. ST3, p. 99, June 1965.
2. Shreir, L. L. Corrosion, Vol. 1. Wiley and Sons, 1963.
3. Brown, B. F. Stress-Corrosion Cracking and Related Phenomena in High-Strength Steels. NRL Rept. 6041, Nov. 6, 1963.
4. Elsea, A. R., and Fletcher, E. E. Hydrogen-Induced, Delayed, Brittle Failures of High-Strength Steels. Defense Metals Information Center Rept. 196, Jan. 20, 1964.
5. McEowen, L. J., and Elsea, A. R. Behavior of High Strength Steels Under Cathodic Protection. Corrosion, Vol. 21, No. 1, p. 28, Jan. 1965.
6. Hanna, G. L., Troiano, A. R., and Steigerwald, E. A. A Mechanism for the Embrittlement of High-Strength Steels by Aqueous Environments. Trans. ASTM, Vol. 57, p. 658, 1964.
7. Hughes, P. C., Lamborn, I. R., and Liebert, B. B. Delayed Fracture of a Low-Alloy Steel in Corrosive Environments. Jour. of the Iron and Steel Inst., Vol. 203, Part 2, p. 154, Feb. 1965.
8. Research Council on Riveted and Bolted Structural Joints. Specifications for Structural Joints Using ASTM A 325 or A 490 Bolts. March 1964.

# *Appendix*

## ANALYSIS OF BOLT STRESS FROM STRAIN GAGES

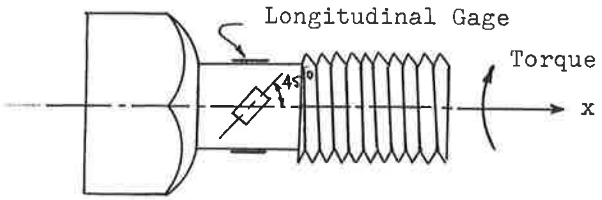


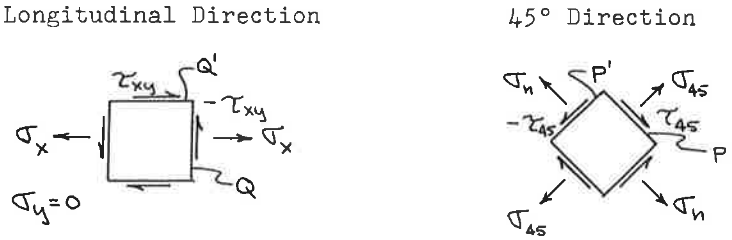


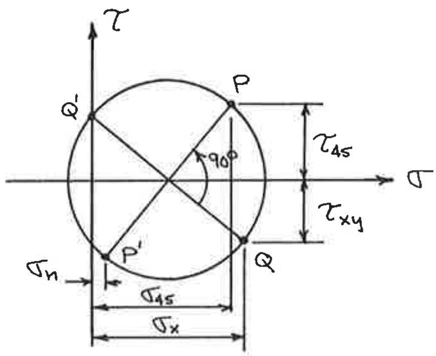


$$\epsilon_x = \frac{\sigma_x}{E} - \frac{\mu \sigma_y}{E}$$

$$\sigma_y = 0$$

$$\epsilon_x = \frac{\sigma_x}{E}$$

$$\sigma_x = \epsilon_x \cdot E$$

$\epsilon_x$ from average (to cancel bending strains) of longitudinal gages.

$$\epsilon_{45} = \frac{\sigma_{45}}{E} - \frac{\mu \sigma_n}{E}$$

From geometry of Mohr's circle diagram:

$$\sigma_{45} = \frac{\sigma_x}{2} + \tau_{xy}$$

$$\sigma_n = \frac{\sigma_x}{2} - \tau_{xy}$$

$$\therefore \; E \cdot \epsilon_{45} = \sigma_{45} - \mu \sigma_n = \frac{\sigma_x}{2} + \tau_{xy} - \mu \left( \frac{\sigma_x}{2} - \tau_{xy} \right)$$

$$E \cdot \epsilon_{45} = \frac{\sigma_x}{2} (1 - \mu) + \tau_{xy} (1 + \mu)$$

$$\text{or} \quad \tau_{xy} = \frac{E \cdot \epsilon_{45} - \frac{\sigma_x}{2} (1 - \mu)}{1 + \mu}$$

$\epsilon_{45}$ from average (to cancel bending strains) of 45° gages.

## General Discussion

JOHN L. RUMPF, Drexel Institute of Technology, and Chairman, Research Council on Riveted and Bolted Structural Joints of the Engineering Foundation—The Research Council on Riveted and Bolted Structural Joints has conducted research on A 490 bolts at several universities during the past several years. On this basis, the Council has written a specification for the use of these bolts in structural connections.

In March 1965, at the annual meeting of the Council, John Macadam delivered a preliminary report on his research relative to the bolt failures at Wolf Creek. At that time the Council set up a committee to investigate the problem of stress corrosion in high strength bolts. No report is available at this time.

The Council also has research on galvanized bolts under way at 2 universities that may be of interest in connection with this problem.

The above remarks are principally informative. The main point to be made, however, is that the Council feels it would be extremely unfortunate if, because of the Wolf Creek incident, the minds of structural engineers were to be prejudiced against the use of A 490 bolts for structural connections.

M. G. SPANGLER, Research Professor of Civil Engineering, Iowa State University, Ames—These papers constitute an important milestone in the search for a sound and workable procedure for the structural design of underground conduits, particularly highway culverts of the flexible type. The authors and their sponsoring agencies are to be congratulated for making this information available to the engineering profession. Too often, in the past, data on failures of this kind have been stamped "confidential," and the profession at large has not been permitted to make independent studies of the phenomena involved. The result has been that the art and science of design of this type of structure has not progressed as rapidly and as far as it might otherwise have done.

The writer has been associated with the extensive research on underground conduits conducted by the Iowa Engineering Experiment Station over the past 40 yr, and has found much of interest in studying the Wolf Creek pipe failure in light of this research. The study leads to the conclusion that the cause of failure of the bolted longitudinal seams can be explained by ordinary garden variety structural mechanics. The longitudinal seam bolts were simply over-stressed in shear and direct tension. It is not necessary to reach far out for a somewhat nebulous hypothesis of corrosion and hydrogen embrittlement of the bolts.

In the first place the value of 105 pcf of the embankment soil, which was used in design, probably was too low by about 20 percent. Because the load on the structure is directly proportional to unit weight of the fill material, the design load was likewise too low. The Marston Theory (5) of loads on underground conduits, which is extensively used in this field of endeavor, is very specific with reference to the linear relationship between load and unit weight. Kraft and Eagle state that the lower value of unit weight was used because of ". . . the anticipated arching action in the rock embankment, and accepted practice in reduced unit weight for culvert design . . . ." It is this writer's opinion that the practice referred to is accepted only to a very limited extent, and that the best and most usual practice is to use the actual unit weight of the overburden soil in culvert design.

The action of the rock fill over the culvert was probably similar to that which would have occurred if the fill had been soil of the same unit weight as the actual fill. In a study of the structural action of 3 cast iron pipe culverts (2) in northeast Iowa made some 35 years ago, the writer arrived at the following conclusion, among others: "There is every evidence that the rock embankments over these culverts acted in a manner entirely analogous to the action of ordinary earth embankments."

Failure of bolts in the longitudinal seams below the spring line was caused by overstress in the bolts under a combination of direct shear, due to tangential thrust in the pipe wall, and tensile stress due to bending moment. The pipe was designed by the Ring Compression Theory. A basic weakness of this theory is its failure to recognize the existence of bending moment in the pipe wall. Actually, there is substantial bending moment around the periphery which must be transferred from one ring plate to the next, along with the tangential thrust, by the longitudinal bolted seam connection. This moment exerts a prying action at the seam, which causes a direct tensile stress in the bolts. This direct tension acts simultaneously with shear in the bolts caused by the tangential thrust. The bolts must be properly spaced and strong enough to resist this composite action.

Calculations of stresses in the bolts have been made using the Marston Theory (5) of loads on conduits and the Spangler Theory (3) of the structural action of flexible pipe culverts. Some of the facts required in the application of these theories are not available and it is necessary to deduce or assume values, based on very limited or nonexistent information. One of these is the height of fill at which the failure began. The evidence indicates that no one had observed the inside of the structure between the time that the fill was at a height of 10 ft above the pipe, which was in November or December 1963, and the time of discovery of the failure, which was in July 1964. The fill height of 83 ft had been completed early in the spring of 1964.

A second important fact, which is unavailable, is the deflection of the pipe at the time failure began to develop. An estimate of this deflection has been made from the plan view of the pipe after discovery of the failure (Fig. 11 of the Kraft and Eagle paper). Here it is indicated that the horizontal diameter of the pipe had increased by approximately 0.9 ft at the locations of the major circumferential seam failures toward each end of the pipe. These points were under fill heights of 34 and 58 ft, respectively. It has been the writer's observation that the deflection of pipes of this kind is roughly proportional to the height of fill at any point. Therefore, assuming that failure occurred at approximately the final height of 83 ft of fill, the deflection may have been in the neighborhood of 20 in.

For purposes of load and strength calculations, the following assumptions are employed:

1. The vertical load on the pipe is uniformly distributed over the top 180 deg.
2. The bottom reaction is uniformly distributed over the bottom 90 deg of the pipe.

3. Passive lateral pressures act against the sides of the pipe. These are distributed parabolically over the middle 100 deg. The maximum unit pressure acts at the spring line and is equal to the modulus of soil reaction multiplied by one-half the horizontal deflection of the pipe and divided by the radius.

A graphical representation of this load system is shown in Figure 1. Further assumptions are:

$H = 83$ ft, $B_c = 18.6$ ft, $\frac{H}{B_c} = 4.47$

$r = 9.3$ ft $= 111.6$ in.

$w = 130$ pcf

$p = 0.9$

$r_{sd} = 0$, $r_{sd}P = 0$, $C_c = 4.47$

$\Delta X = 20$ in.

$E = 30,000,000$ psi

$I = 0.226$ in. 4/in., $EI = 6,780,000$ in.

$D_l = 1.0$

$K = 0.096$

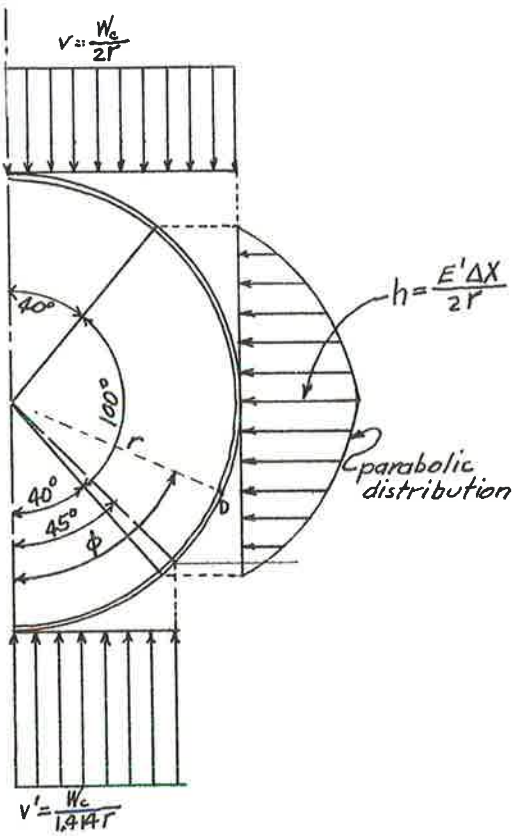


Figure 1. Assumed load system on Wolf Creek culvert.

Calculation of load on the pipe by the Marston formula,

$$W_c = C_c w B_c^2 \tag{1}$$

$$W_c = 4.47 \times 130 \times 18.6^2 = 201,000 \text{ plf}$$

Calculation of modulus of soil reaction by the Spangler formula,

$$\Delta X = D_l \frac{KW_c r^3}{EI + 0.061E'r^3} \tag{2}$$

$$E' = 1240 \text{ psi}$$

$$h = \frac{E'\Delta X}{2r} = \frac{1240 \times 20}{2 \times 111.6} = 111 \text{ psi}$$

The units of h are pounds per inch of circumference, per inch length of pipe.

The equations for bending moment, $M_D$, and tangential thrust, $R_D$, in the pipe wall are most conveniently written separately for the vertical and horizontal loads (3).

For vertical loads these are:

When $\phi$ lies between 0 and 45 deg

$$M_D = W_c r\,(0.183 - 0.26\cos\phi - 0.354\sin\phi) \tag{3}$$

$$R_D = W_c\,(0.026\cos\phi + 0.707\sin^2\phi) \tag{4}$$

When $\phi$ lies between 45 and 90 deg

$$M_D = W_c r\,(0.36 - 0.026\cos\phi - 0.5\sin\phi) \tag{5}$$

$$R_D = W_c\,(0.026\cos\phi + 0.5\sin\phi) \tag{6}$$

When $\phi$ lies between 90 and 180 deg

$$M_D = W_c r\,(0.110 - 0.026\cos\phi - 0.25\sin^2\phi) \tag{7}$$

$$R_D = W_c\,(0.026\cos\phi + 0.5\sin^2\phi) \tag{8}$$

For horizontal pressure loads, the equations are:

When $\phi$ lies between 0 and 40 deg

$$M_D = hr^2\,(0.345 - 0.511\cos\phi) \tag{9}$$

$$R_D = hr\;0.511\cos\phi \tag{10}$$

When $\phi$ lies between 40 and 140 deg

$$M_D = hr^2\,(0.199 - 0.5\cos^2\phi + 0.143\cos^4\phi) \tag{11}$$

$$R_D = hr\,(\cos^2\phi - 0.568\cos^4\phi) \tag{12}$$

When $\phi$ lies between 140 and 180 deg

$$M_D = hr^2\,(0.345 + 0.511\cos\phi) \tag{13}$$

$$R_D = hr\;0.511\cos\phi \tag{14}$$

Evaluation and combination of these equations yield the moment diagram shown in Figure 2, and the tangential thrust diagram of Figure 3. The maximum moment in the pipe wall is 63 ft-kips per foot at the bottom. The moment at the longitudinal seam near the lower quarter point ($\phi = 45°$) is approximately 40 ft-kips. A section through the seam is shown in Figure 4. Since the seam must transmit moment from one plate to another, we may determine the tension in the bolts by writing moments about the point of rotation of the seam and setting this equation equal to the moment in the wall.

A difficulty arises in trying to identify the fulcrum or point of rotation, and present knowledge does not permit a rational selection of the actual point. However, it is at least possible that rotation might occur about the inner row of bolts, and since the rows were only 2 in. apart, the tension in the outer row would be 40 ÷ 0.167 = 240 kips per ft. Since there are 4 bolts per ft in the outer row, the tensile stress in each bolt is 60 kips. ASTM A 354BD bolts, ¾-in. diameter, have a minimum specified ultimate strength of 50.1 kips. Therefore it is probable that failure of the structure began by tensile failure of the bolts in the lower quarter point seams. Since the calculated stress in the bolts is greater than the minimum specified strength, the factor of safety is less than unity. This suggests that failure probably occurred at some height of fill less than the maximum of 83 ft above the culvert.

This failure hypothesis ignores the possibility that shear stress in the bolts may have contributed to the initial failure. The tangential thrust at the seam in question is approximately 125 kips per ft of pipe, or 15.6 kips per bolt. It is possible that the initial torque to which the bolts were subjected during construction may have created enough

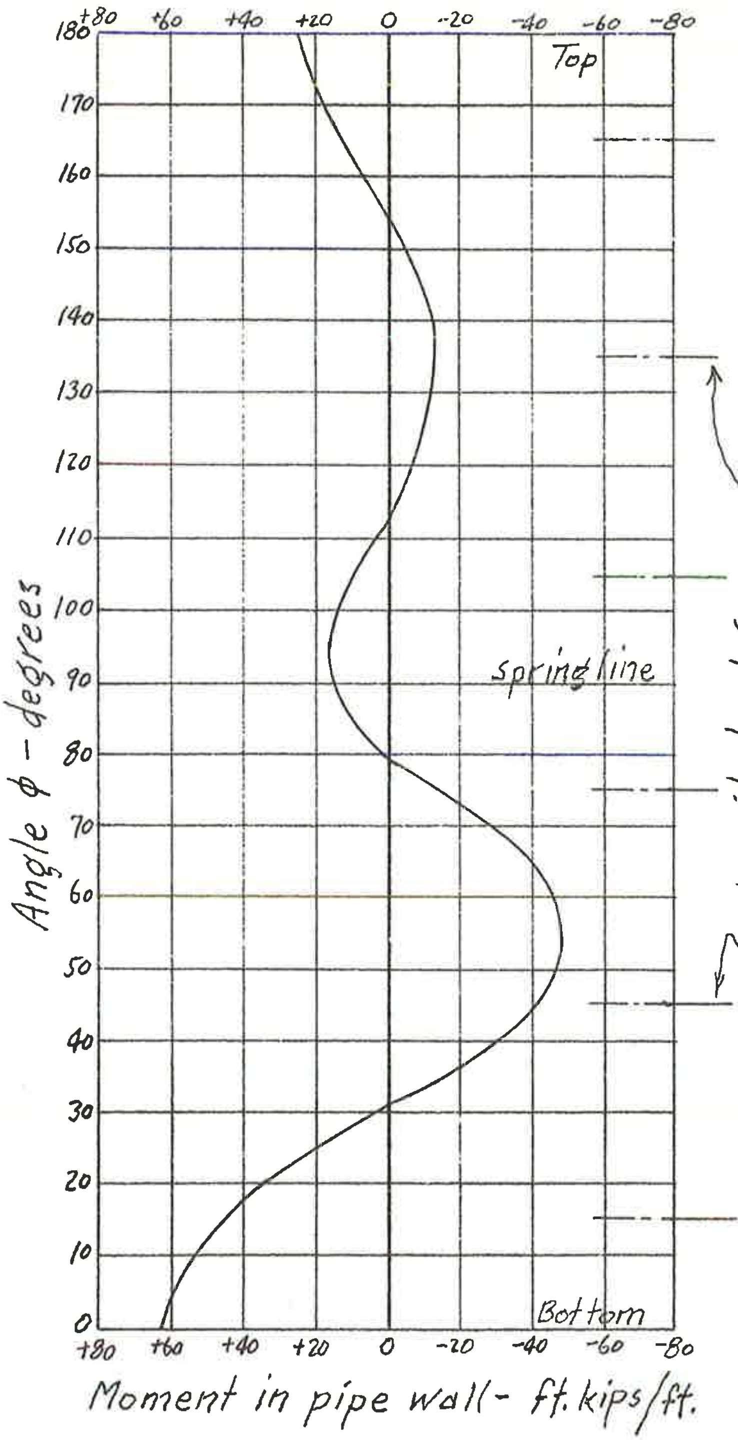


Figure 2. Moment diagram—Wolf Creek culvert.

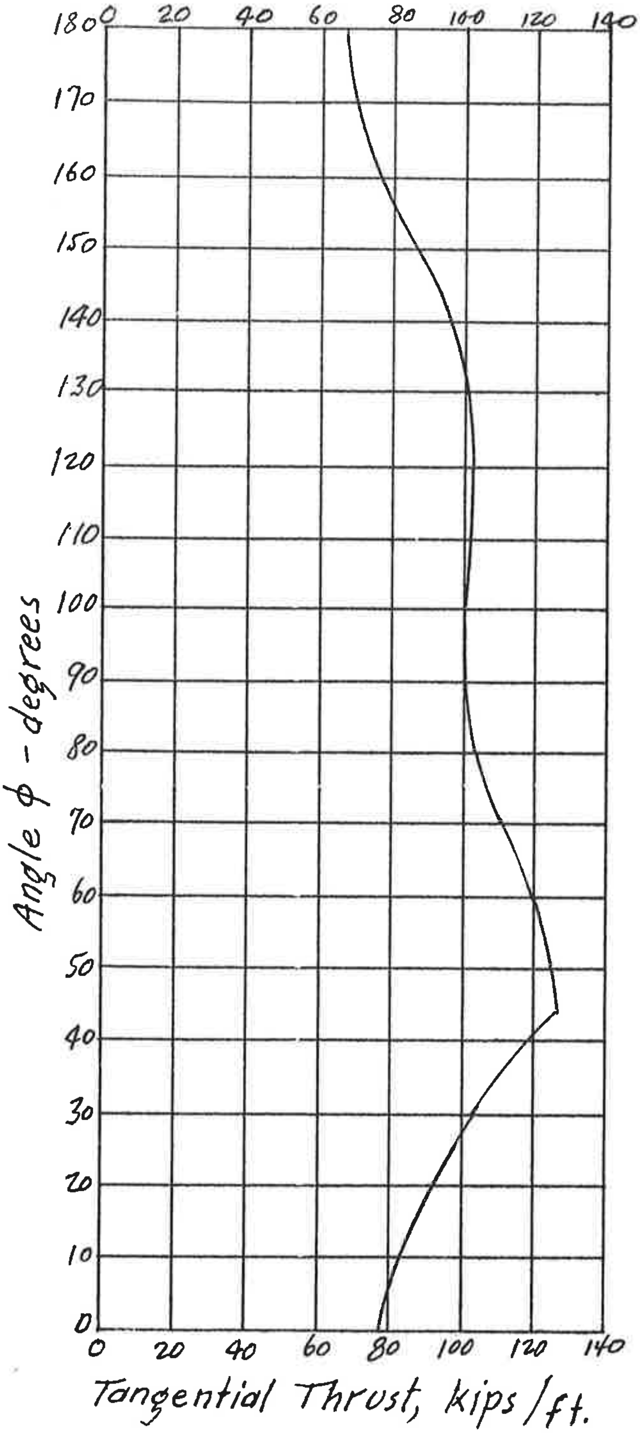


Figure 3. Thrust diagram—Wolf Creek culvert.

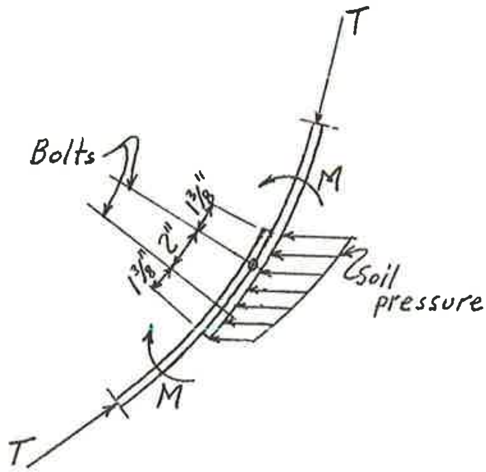


Figure 4. Forces on bolted seam—Wolf Creek culvert.

frictional resistance between the plates to carry this amount of thrust without stressing the bolts in shear. However, as bending moment developed, this frictional resistance would be relieved by the prying action of the moment. The magnitude of this relief is not readily determinable. If this transfer of shearing resistance from friction between the plates to shear stress in the bolts occurred, the composite effect of shear and tension in the bolts would have entered into the bolt failure phenomenon. Some recent research at the University of Illinois (1) has contributed materially to understanding of the failure of high strength bolts under composite stress conditions.

An important result of this analysis is the demonstration that the maximum stressed longitudinal seams are located in the quadrants below the springline (Figs. 2, 3). This is the region of extensive bolt failures as shown in Figure 2 of the Macadam paper.

In the above analysis it was assumed that the load on the pipe was equal simply to the dead weight of the prism of soil directly above the structure. This is tantamount to assuming that the product of the projection ratio and the settlement ratio was equal to zero (5, Chap. 24). The projection ratio is defined as the ratio of the distance which the top of the pipe projects above the natural ground surface to the horizontal dimension of the pipe. It apparently was about 0.9 in this case, as indicated in Figure 11 of the Kraft and Eagle paper.

The settlement ratio is a function of the relative settlement between the top of the pipe and the critical plane of the soil fill at the sides of the pipe, i.e., the horizontal plane which was originally level with the top of the pipe when construction of the fill began H = 0. If the critical plane settles more than the top of the pipe, shearing forces develop along the vertical sides of the central prism of soil, which are directed downward. The settlement ratio in this circumstance is positive and the load on the pipe is greater than the weight of the central prism.

If the critical plane settles less than the top of the pipe, the settlement ratio is negative, the shearing forces are directed upward, and the load on the pipe is less than the weight of the prism. A neutral or transition case occurs if the top of the pipe and the critical plane settle the same amount. The settlement ratio equals zero, there are no shearing forces, and the load on the pipe is simply equal to the weight of the central prism of overburden soil.

Some field measurements of settlement ratios of highway culverts were made by the writer prior to World War II (4). Most of the culverts studied were of the rigid type, but measurements were made on 4 corrugated steel culverts. Of these, the measured values of settlement ratio of 3 of the pipes were practically zero. However, on the fourth pipe the measured value was +0.8. This is a very small sample and general conclusions relative to settlement ratios which develop in connection with flexible culverts are not justified. However, they do indicate that under some circumstances, the settlement ratio for a flexible pipe installation can be a relatively high positive value, and the load on the pipe can be substantially greater than the weight of the overlying prism of soil.

If this situation prevailed in the Wolf Creek installation, the conditions of load and supporting strength analyzed above for an 83-ft hill could have developed at fill heights considerably below 83 ft. To illustrate, assume settlement ratios of +0.22 and +0.78 (products $r_{sd}P$ = +0.2 and +0.7). The estimated load of 201 kips per lineal ft might have occurred at fill heights of 63 ft and 54 ft, respectively, under these assumed circumstances.

Kraft and Eagle state that an imperfect ditch environment was created during reconstruction of the culvert by placing a layer of baled straw to a depth of 5 to 7. 5 ft above the pipe and a 6-ft layer of loose soil above the straw. Also, ⅞-in. ASTM A 325 bolts were used to replace the ¾-in. A 354 bolts. The writer estimates that the imperfect ditch construction will reduce the vertical load on the pipe from 201 klf to about 139 klf, or 31 percent. The strength of the bolts in tension will be increased from 50. 1 to 55. 5 kips, or nearly 11 percent. It is probable that the reconstructed culvert will safely carry the load of the embankment, but the factor of safety of the bolted seams will be substantially less than 3. 5, the factor which was intended for the original design.

## Conclusions

The writer's analysis of the structural failure of the Wolf Creek culvert leads to the following conclusions:

1. Failures of the longitudinal bolted seams were caused by a combination of using a design load which was too low, plus inadequate strength and spacing of bolts to carry the composite direct tension and possible shear stress to which they were subjected.
2. The designers state that the unit weight of the overlying embankment material ". . . could be expected to be 130 lb per cu ft or more." However, they used a unit weight of 105 pcf in calculating the design load, whereas the Marston Theory of loads on underground conduits indicates that the actual unit weight should be used.
3. The culvert was designed by the Ring Compression Theory. A major weakness of this theory is its failure to recognize the existence of bending moment in the pipe wall. Actually, there is substantial bending moment around the periphery of a flexible pipe culvert. The function of a longitudinal seam in the wall is to transmit both the bending moment and the tangential thrust from one ring plate to the next.
4. Calculations of direct tensile stress in the seam bolts due to prying action accompanying transmittal of bending indicate that the bolts were stressed beyond their ultimate strength. Failure of the bolts was inevitable.
5. Both bending moment and tangential thrust are greater in the lower quadrants. This accounts for the fact that practically all bolt failures occurred in the lower quadrants.
6. The designers used a settlement ratio equal to zero in calculating the design load. There is a possibility that the settlement ratio may have been greater than zero, which would have increased the load beyond the dead weight of the prism of embankment material directly over the culvert.
7. Lack of knowledge concerning the actual settlement ratio plus uncertainty relative to the action of a 2-row bolted seam in transmitting bending moment, lead the writer to believe it is probable that failure of the bolted seams began at a height of fill substantially less than the final height of 83 ft. The height at which failure began may have been as low as 50 or 60 ft.
8. The utilization of the imperfect ditch method during reconstruction of the embankment over the repaired culvert, plus the use of ⅞-in. A 325 bolts apparently will produce a safe structure. However, the factor of safety will probably be substantially less than the factor of 3. 5 aimed at in the original design.

## References


1. Chesson, Eugene, Jr., Faustino, N. L., and Munse, W. H. High-Strength Bolts Subjected to Tension and Shear. Jour. Struct. Div., Proc. ASCE, Oct. 1965.
2. Spangler, M. G. Investigation of Loads on Three Cast Iron Pipe Culverts Under Rock Fills. Bull. 104, Iowa Eng. Exp. Sta., 1931.
3. Spangler, M. G. The Structural Design of Flexible Pipe Culverts. Bull. 153, Iowa Eng. Exp. Sta., 1941.
4. Spangler, M. G. Field Measurements of the Settlement Ratio of Various Highway Culverts. Bull. 170, Iowa Eng. Exp. Sta., 1950.

5. Spangler, M. G. Soil Engineering, 2nd Ed. International Textbook Co., Scranton, Pa., 1960, 483 pp.
6. Watkins, R. K., and Spangler, M. G. Some Characteristics of the Modulus of Passive Resistance of Soil: A Study in Similitude. HRB Proc., Vol 37, p. 576, 1958.

JOHN N. MACADAM, Closure—The author appreciates Rumpf's concern for possible interpretations of a paper which might prejudice engineers against the use of A 490 bolts for structural connections. The paper was concerned only with "A 490-type" bolts used in structural plate culvert pipe, which is a limited and perhaps unique application. It should be strongly emphasized that neither the geometric configuration nor the field application of these bolts corresponds to traditional high strength bolting uses, i.e., building and bridge construction. The conclusions reached in the paper must not be interpreted as dissatisfaction with the performance of high strength bolts used for conventional structural joints, either friction or bearing-types. The good performance of such joints is a matter of common knowledge gained over a period of years. The work of the Research Council on Riveted and Bolted Structural Joints has greatly contributed to the favorable usage of high strength bolts.

It is encouraging to know that the Research Council has recently initiated investigations on problems of stress corrosion of high strength bolts and also on galvanized bolts. Through the auspices of organizations such as the Research Council, a better understanding of structural bolt behavior in corrosive applications can be attained.

Spangler's remarks are directed jointly to the author's paper and the companion paper by Kraft and Eagle. Spangler's study of the field failure is a worthy contribution to the papers. Although a hydrogen-stress cracking hypothesis is probably uncommon to those concerned with highway culvert performance, this type of phenomenon in high strength steel has been known for some time and is well documented (1, 2, 3, 4). It is known that a level of sustained tensile stress and a hardness comparable to the failed bolts at Wolf Creek, together with a source of nascent hydrogen, can cause failure.

Spangler has concluded that the A 490 bolts in the longitudinal seams failed due to over-stressing in a combination of direct tension from transferal of bending moment in the pipe wall and shear from thrust transferal. In the chronological development of the author's investigation, static strength tests were made initially in an effort to explain the field failure by a mechanical weakness of the bolts or an overstressed state. It was only after the static load experiments failed to resolve the failures that environmental effects were investigated.

As pointed out in the paper, only A 490 bolts failed. For all practical purposes the failures extended up to locations in the pipe where A 325 type bolts were used. If overloading had been the cause of failure, it would seem likely that some A 325 bolts adjacent to the A 490 bolts would have also failed, and in a ductile manner. Bolt fracture surfaces generally resembled the brittle fracture surfaces from the laboratory hydrogen-stress cracking experiments more than typical combined shear-tension failures.

Using all of Spangler's assumptions for the conditions at Wolf Creek, together with his well-known method of elastic analysis, resulted in a moment of 480 in.-kip per ft for the critical longitudinal seam. However, the maximum moment capacity of the ⅜-in. structural plate by tests is only 143 in.-kip per ft, as given in Table 3 of the paper. Spangler's computed value of 480 in.-kip per ft is therefore a moment which cannot be developed by the pipe wall. Hence, his deduction that 60 kips per bolt would be developed in direct tension does not follow.

A rational analysis of the bolted lap seam subjected to moment is shown in Figure 1. For a moment of 143 in.-kip per ft acting on the seam, bolt tensions of 9,200 lb/bolt and 3,400 lb/bolt are obtained for the outer and inner bolt rows, respectively. This analysis is based on a condition of no initial bolt tension from tightening. Actually, with

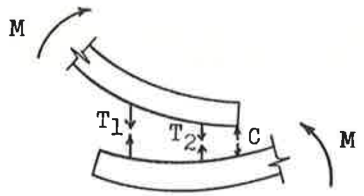


From $\Sigma$ M equation and compatibility of deformations equation the bolt tensions $T_1$ and $T_2$ can be determined:

$$3.375\, T_1 + 1.375\, T_2 = M$$

$$T_1 = 3.109\, T_2 - 0.0372\, M$$

$$T_1 = 0.2577\, M$$

$$T_2 = 0.09483\, M$$

for M = 143,000 in.-lb per ft

$T_1$ = 36,800 lb for 4 bolts or 9,200 lb/bolt

$T_2$ = 13,600 lb for 4 bolts or 3,400 lb/bolt

Figure 1. Analysis of ⅜-in. structural plate lapped seam subjected to moment.

initial prestress in the joint, the bolt tensions are for all practical purposes unchanged until the tension from external loading exceeds the initial tension.

The combination of 9,200 lb maximum possible direct tension and Spangler's value of 15,600-lb shear can be compared to the results obtained by Chesson et al. (5). Figure 2 shows the combined load state for the structural plate bolts as related to an interaction curve from tests on ¾-in. A 354 BD (A 490) bolts with threads in the shear plane. A factor of safety against failure of approximately 1.7 exists.

It is recognized that the ring compression method predicts that installed culvert pipe performance can be based on pipe wall thrusts. Some bending moment does exist in the pipe wall, but a history of properly backfilled installations has shown that the ring compression method is a successful design approach. Spangler's method of analysis for computing bending moments apparently can sometimes result in values which cannot be resisted by the pipe wall. In the case of the Wolf Creek structure, such computed moments lead to a false hypothesis of the bolt failures.

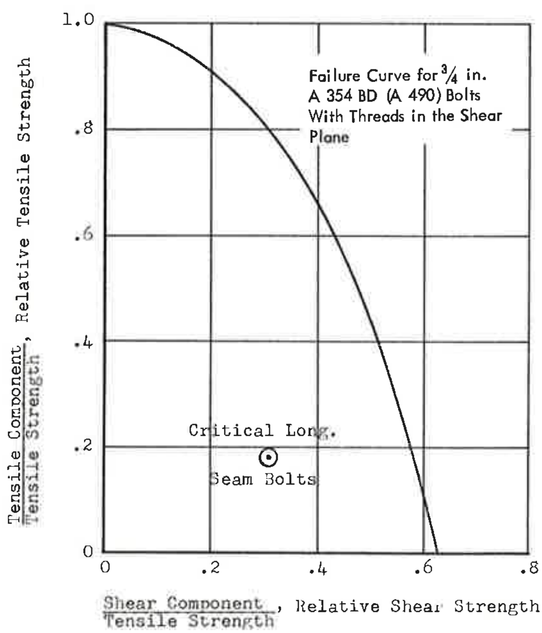


Figure 2. Comparison of critical longitudinal seam bolts and interaction failure curve from Illionis tests (Fig. 4 of Ref. 5).

References

1. Frohmberg, R. P., Barnett, W. J., and Troiano, A. R. Delayed Failure and Hydrogen Embrittlement in Steel. ASTM Trans., Vol. 47, p. 892, 1955.
2. Johnson, H. H., Morlet, J. G., and Troiano, A. R. Hydrogen, Crack Initiation and Delayed Failure in Steel. Trans. Met. Soc., AIME, Vol. 212, p. 528, 1958.
3. Elsea, A. R., and Fletcher, E. E. Hydrogen-Induced, Delayed, Brittle Failures of High-Strength Steels. Defense Metals Information Center Rept. 196, Jan. 20, 1964.
4. McEowen, L. J., and Elsea, A. R. Behavior of High Strength Steels Under Cathodic Protection. Corrosion, Vol. 21, No. 1, p. 28, Jan. 1965.
5. Chesson, E., Jr., Faustino, N. L., and Munse, W. H. High-Strength Bolts Subjected to Tension and Shear. Jour. Struct. Div., ASCE Proc., Vol. 91, No. ST5, p. 155, Oct. 1965.

HAROLD L. EAGLE, Closure—Professor Spangler implies that from his experience the earth load on a buried pipe in a rock fill can be expected to be as large as the weight of the entire soil mass directly over the pipe. The design of the original pipe did recommend the use of an imperfect trench fill. In reviews of the design, this recommendation was eliminated as being unnecessary. The rebuilt pipe has been constructed with the imperfect trench method using a 30-in. layer of hay a short distance above the pipe and the same width as the pipe. This fill has been completed for over 3 months. Instrumentation of the installation by Montana State University is functioning quite well. This instrumentation indicates roughly 60 percent of the weight of the fill directly over the pipe is presently being supported by the pipe. We expect there will be some increases in this percentage in the years ahead. We admit construction without the imperfect trench method would be expected to produce greater loads on the pipe. However, as presently constructed, it is our opinion the load on the pipe will remain substantially less than the entire weight of the fill over the pipe. This was the original basis for design.

Professor Spangler in his discussion considers a vertical deflection of the pipe of 20 in. when failure occurred. Evaluation of the pipe dimensions after failure for the entire length of the pipe indicates the vertical deflection at the time of failure was about one foot, and that the increase from initial shape in horizontal diameter was about 0.6 ft. We made moment calculations for the indicated distorted shape assuming an entirely "elastic" condition. This analysis did indicate a moment of about 27 kip ft per ft near the lower quarter points and higher moments at the bottom. However, evaluation of the yield moment of the pipe section for a "plastic" condition using a steel stress of 35,000 to 40,000 psi reveals that the pipe shell cannot resist a moment of over 11 to 13 kip ft per ft. Actual bending tests have shown the plastic hinge moment for the section to be 11 to 12.5 kip ft per ft.

Professor Spangler's consideration of a moment of 63 kip ft per ft is therefore not valid. The deflection assumed is about twice that which occurred at failure and plastic hinges in the pipe shell limited the maximum moment to about 11 or 12 kip ft per ft.

We did make a theoretical analysis of bolt stresses including direct tensile stresses, torsional stresses, shear stresses, and bolt tensile stresses due to bending in the joint. When these stresses are combined and maximum tensile and shear stresses computed, values are obtained approaching yield point stresses for the high strength bolt material. We do not feel these theoretical analyses tell the whole story. We have used hot driven rivets successfully for years, yet every good rivet reaches its yield stress in cooling. The rivets still carry large added shear and tensile loads. We have concluded that actual joint tests are essential to evaluate joint adequacy.

Mr. Macadam reports on extensive physical testing of the bolted joints in his paper. Figures 8, 9, 10, 11 and 12 in that report show photographs of shear and bending tests which were constructed with varying amounts of bolt torque. We believe Macadam's statement is well founded by the laboratory tests of joint strength: "No evidence of bolt or joint weakness was observed in any of the static strength tests made in the laboratory in search of a plausible explanation of field failure."

## Conclusion

I do agree with Prof. Spangler that the structural plate pipe may have been subjected to greater than design loads. If so, based on data received from instrumentation of the rebuilt pipe, any overload which occurred was probably due to the elimination of the imperfect fill method recommended by the original design. I strongly disagree with Spangler's conclusion that longitudinal seam strength was too low. The physical testing of the joint has demonstrated that normally the pipe shell would yield prior to a joint failure. I feel that the hydrogen-stress cracking explanation set forth in Macadam's paper does appear to be a major factor to consider in evaluating the failure of the Wolf Creek Pipe.